Newcastle University

School of Biology

The effect of salinity and shaking on growth, and lipid biosynthesis-related gene expression in *Parachlorella kessleri*

Ilgaz Cakin

Student Number : 160561616

MSc Industrial and Commercial Biotechnology

Supervisor : Dr Ethan Hack

Word count: 10698 (excl. tables, and figure legends)

Date: 15.08.2017

DECLARATION

a) I declare that this thesis is my own work and that I have correctly acknowledged the work of others. This submission is in accordance with University and School guidance on good academic conduct.

b) I certify that no part of the material offered has been previously submitted by me for a degree or other qualification in this or any other University.

c) I confirm that the word length is within the prescribed range as advised by my school and faculty.

d) Does the thesis contain collaborative work, whether published or not? Yes / No

If it does please indicate what part of the work is your independent contribution on a separate sheet.

Signature of Candidate ..... Date 15.08.17.

List of Abbreviations

accD – gene for acetyl co-A carboxylase beta subunit

ACP – acyl carrier protein

CAGR – Compound average growth rate

DAG – diacylglycerol

DGAT – diacylglycerol O-acyltransferase

FA – Fatty acid

FAS – Fatty acid synthase

FAT – Fatty acyl thioesterases

FFA - Free fatty acid

G3P – Glycerol- 3- phosphate

KEGG – Kyoto encyclopedia of genes and genomes

LACS – Long-chain acyl-CoA synthetase

LPA - lysophosphatidate

LPAAT – lysophosphatidic acid acyltransferase

TAG – triacylglycerol

Abstract

Among microorganisms, some microalgae have a very high potential of producing lipid rich contents which are suitable for renewable energy production. These lipid contents can be converted to biofuels such as biodiesel and they can be a good alternative to fossil fuels. *Parachlorella kessleri*, a stress tolerant chlorophyte microalga, is capable of reaching very high biomass, starch, and lipid productivity levels. In order to enable the economical, ecological and efficient production of lipids by *Parachlorella kessleri*, new growth optimization strategies should be researched. The objective of this experiment is to investigate the effect of salinity and shaking on growth, and lipid biosynthesis-related gene expression in *Parachlorella kessleri.*

Salinity tolerance was tested by growing cells on 3N-BBM+V with different concentrations of NaCl, chlorophyll was assayed in order to measure growth. Shaking tolerance was tested by growing cells on rotary. Lipid analysis was done in order to quantify and characterize the lipids. In all samples, the cellular growth rate which was was parallel to the total chlorophyll growth rate. *Parachlorella kessleri* was found unable to grow optimally on high salt Bold Basal Medium (3N-BBM+V) which contains 0.6 M NaCl, same as the sea water. The algal culture on no salt 3N-BBM+V had the highest growth rate. Low salt culture (0.15 M NaCl) had the second highest growth rate. Medium salt culture (0.3 M NaCl) had the third highest growth rate. When cultures in different salinity were cultivated on rotary, the range was the same; the highest growth rate on no salt 3N-BBM+V, second on low salt 3N-BBM+V and third on medium salt 3N-BBM+V.

Shaking algal cultures on no salt 3N-BBM+V gave a higher growth rate than no salt still cultures. On the other hand, it was found that the growth rate of medium salt shaking culture was higher than the growth rate of medium salt still culture. In order to investigate the acclimation trends, cells were transferred to different media in different salinity. Cells transferred from the low salt 3N-BBM+V to the high salt 3N-BBM+V and cells transferred from the no salt 3N-BBM+V to the high salt 3N-BBM+V were unable to acclimate; thus they were unable to grow optimally. There was no remarkable change in the growth rates of algal cells transferred from the high salt to the no salt 3N-BBM+V and cells directly cultivated on the no salt 3N-BBM+V.

RT-qPCR analysis indicated 2.6 fold higher expression of the *accD* gene and 4 fold higher expression of the *rbcL* gene of low salt still 3N-BBM+V culture compared to no salt still 3N-BBM+V culture. Relative expression of the *accD* gene of no salt still 3N-BBM+V culture was 3.4 fold higher compared to medium salt still 3N-BBM+V culture. Relative expression of the *accD* gene of no salt still 3N-BBM+V culture was 2.7 fold higher compared to high salt still 3N-BBM+V culture. There was no significant change in *accD* and *rbcL* expression of no salt still or shaking 3N-BBM+V culture. When cultures in different salinity were cultivated on rotary, relative expression of the *accD* and *rbcL* genes of no salt shaking 3N-BBM+V culture was 7.4 fold higher compared to low salt shaking 3N-BBM+V cultures. In contrast, medium salt shaking 3N-BBM+V culture displayed 2.7 fold higher expression of the *accD* gene and 3.8 fold higher expression of the *rbcL* gene compared to no salt shaking 3N-BBM+V culture. It was found that the relative expression of the *accD* and *rbcL* genes of the cells transferred from high salt to no salt 3N-BBM+V were 2 fold higher compared to the cells transferred from low salt to high salt 3N-BBM+V.

Lipids which were extracted by the Folch method and quantified by the thin layer chromatography (TLC) showed evidence of fatty acids and triacylglycerols in all algal cultures. Medium salt shaking culture had the highest fatty acid and triacylglycerol content among all shaking algal cultures. Low salt shaking culture had the second highest fatty acid and triacylglycerol content. No salt shaking culture had the least fatty acid and triacylglycerol content. On the other hand, no phospholipid or glycolipid was detected in any algal sample.

For further studies, it is recommended to investigate more genes relevant to lipid metabolism and extend the environmental stress duration in order to see time dependent gene expression profile on a wider scale. In addition, a wider range of medium salinity and shaker rpm can be tested to obtain more detailed results.

1.Introduction

Although their use drives climate change, fossil fuels are widely used to meet the energy requirement of the modern world and the demand has been rising for years in order to catch up the industrial growth. According to the World Bank, between 2000 and 2014, the compound average growth rate (CAGR) of fossil fuel energy consumption is 0.08 percent (OECD/IEA, 2014). In addition, between the same time interval, the compound average growth rate (CAGR) of energy use (kg of oil equivalent per capita) is 1.1 percent. (OECD/IEA, 2014). Crude oil consumption rate is 4 billion tonnes a year (CIA, 2017). According to the CIA projections, total known oil reserve will end by 2052. The total gas reserve can fill the gap of crude oil depletion for just 8 years, taking us to 2060. The richest reserve is coal, can be enough until 2088 (CIA, 2017). Low research and development requirements, easy accessibility and economic advantage of fossil fuels have satisfied investors and

governments for a long time. However, damage of fossil fuels to the environment, rising costs due to limited supply and increasing demand have triggered the search for alternative energy.

1.1 Biofuels

Biofuels are one of the major invested alternative energy sources. They meet 1.6 percent of global liquid energy demand (World Energy Council, 2016). The United States, Brazil, and Europe are the major producers of biofuels (World Energy Council, 2016). In 2017, The European Parliament approved legislation in order to increase the first-generation biofuel consumption up to 7 percent of total energy consumption in transport by 2020 (European Commission, 2017). Biofuels are produced through biological processes either in nature or specific bioreactors. Biofuels are mainly separated as bioalcohols, biodiesel, green diesel, biofuel gasoline, vegetable oil, bioethers, biogas, syngas and solid biomass fuels (Rostek et al., 2012). Since biodiesel contains less carbon and more hydrogen and oxygen content than fossil diesel, it has improved combustion rate, yet lower unburnt carbon emission. Furthermore, biodiesel is biodegradable and nontoxic (Moser et al., 2009). Biodiesel, which consists of long-chain methyl, ethyl, or propyl esters can be produced from waste cooking oil, animal fat and oil crops such as mustard, flax, jatropha, soy, rapeseed, sunflower and mahua by transesterification, but the production cannot be sufficient for the demand for transport fuels (Moser et al., 2009).

1.2 Microalgae

Microalgae, also called microscopic algae, appear one of the most promising contributors for the next generation high energy biofuel production such as biodiesel. Algal oils are used as precursor molecules for biodiesel production. These unicellular photosynthetic microorganisms are capable of converting carbon dioxide into carbon-rich lipids which are structurally very close to biodiesel (Chisti, 2007). These microorganisms are found in freshwater and marine systems. It has been estimated that 200,000-800,000 microalgae species exist, yet only 50,000 species are described (Cheng et al., 2011). Their size varies from a few micrometres (μm) to a few hundred micrometres (Cheng et al., 2011). Some microalgae can grow very rapidly and their cellular structure is rich in oil. Studies show that microalgae species have a quite common oil levels of 20–50% (Chisti, 2007). Plants can use sunlight to produce oils as well, but microalgae do it more efficiently than crop plants (Chisti, 2007). On the other hand, many optimization processes such as strain selection, methods of systems biology, process engineering and genetic engineering are needed to make algal biofuels economically and practically feasible for bulk applications.

1.3 Microalgae cultivation

There are some main points to take into account in order to cultivate microalgae efficiently. These points are: minimizing space requirements, reducing capital and production costs, minimizing contamination, controlling cultivation conditions, and efficient provision of carbon dioxide and light (Mata et al., 2010). There are two major cultivation systems used for the photoautotrophic production of microalgae: open pond and closed photobioreactors (Borowitzka, 1999).

Open pond systems consist of minimum 4000 square metres in size ponds. Algae inside the pond water are exposed to sunlight to trigger photosynthesis and biomass conversion. Open pond systems have a lower operational expenditures and easier scaling up compared to the closed systems, but major drawbacks cause a shift to focus on the closed biosystems. First of all, large scale production of algal species is a big challenge; a very tiny amount of contamination can cause inhibition of reactions. Evaporative losses and incapability of temperature control disrupt the sustainability of the system. A large area of land usage is another drawback. In addition, CO_2 is not used efficiently and harvesting cost is still high (Borowitzka, 1999).

Closed bioreactors are specialized vessels in which raw materials are biologically converted into specific products by using microorganisms such as microalgae. Bioreactors are capable of maintaining the specific environment for microorganisms to provide optimum growth conditions. The specificity of the environment is determined by temperature, pH, substrate, salts, vitamins, and O_2. Unlike open-air systems, closed photobioreactors are used to cultivate single species of microalgae. Photobioreactors have tubular or flat plate structures depending on the process. On the other hand, closed bioreactors have some problems too. Scaling up is a major challenge because the bioreactor volume depends on a diameter or thickness of a plate which causes the need for a larger area. The second drawback is the operational costs of closed systems which are more expensive than the operational costs of open systems (Borowitzka, 1999, Chrismadha and Borowitzka, 1994).

1.4 Bold Basal Medium with 3-fold Nitrogen and Vitamins

There are many different kinds of algal growth medium which provide specific growth conditions for algae species. 3N-BBM+V is a nitrogen and vitamin rich growth medium which is suitable for freshwater algae cultivation (Brown and Bold, 1964). In this experiment, 3N-BBM+V was used. The original form of the Bold's basal medium does not contain vitamins. In this experiment, some vitamins were added into the media to provide robust algal growth. Vitamin B_{12} takes an active role in DNA, fatty acid, and amino acid metabolism. Vitamin B_1 functions in metabolic processes such as degradation of sugar and amino acids (Depeint et al., 2006). In 3N-BBM+V, sodium nitrate provides the nitrogen requirement of the microalgae in order to proceed its growth and biochemical reactions (Li et al., 2008). Calcium chloride prevents mineral deficiency by providing the calcium and chloride requirement of the algae (Yocum, 2008). Magnesium sulphate is another major salt used in 3N-BBM+V to provide magnesium and sulfur to microalgae (Singh et al., 2011). Together with monopotassium phosphate, dipotassium phosphate provides buffering (Reuveni et al., 1996). Sodium chloride provides sodium and chloride minerals to algae and enables the ideal salinity for growth. Trace elements iron (II) sulphate, manganese (II) sulphate, zinc sulphate, copper (II) sulphate, cobalt (II) sulphate and molybdic acid sodium salt dihydrate are essential for algal metabolism (Rupérez, 2002).

1.5 Visualization of Lipids in microalgae

Lipophilic stains are used to visualize lipid bodies in microalgae (Cirulis et al., 2012). Nile red (9-diethylamino-5H-benzo[α]phenoxazine-5-one) is a widely used lipophilic stain which can dye intracellular lipid molecules and gives them yellow color under fluorescence. In apolar conditions, the 9-diethylamino substituent of the molecule

gives an electron to the carbonyl group across the ring via the process called electron delocalization. This process causes the light emission visible under a fluorescent microscope (Jose et al., 2006).

1.6 Microalgae responses under salt stress or shaking

The effect of salinity on *Dunaliella salina* cells was studied before. *D. Salina* is a green micro-algae especially found in sea salt fields. Takagi et al. (2006) reported that 1.0 M NaCl concentration resulted in a higher lipid content in *D. Salina* than 0.5 M NaCl concentration. In addition, it was inferred that 1.5 M NaCl concentration was lethal for *Dunaliella salina* cells. Another study displayed the effect of salinity on freshwater microalgae *Chlamydomonas mexicana* and *Scenedesmus obliquuswere* up to 0.1 M. Salama et al. (2013) inferred that lipid accumulation parallelly increased when the salinity of the BBM was increased from 0 to 0.025 M. Furthermore, Kaewkannetra et al. (2012) found that oil accumulation of *Scenedesmus obliquus*, *S. armatus* and *S. Bernadii* was higher in 0.3 M NaCl concentration than 0.05 M and 0.2 M NaCl.

Physiological mechanism during salinity stress should be focused on in order to understand the lipid accumulation response. Researchers assume that coping mechanisms for the osmotic stress enable a higher lipid accumulation in algal cells. Salinity dependent osmotic stress mainly interferes with the ion transport regulation mechanism of the cells. Osmotic stress disturbs membrane structure via 3 probable mechanisms: tension caused anisotropic changes, electro-mechanical compression of the membrane and stretch-activated ion channels. Membrane disturbance causes changes in K^+ , Na^+ and Cl^- concentrations of the cell. Some microalgae may adapt to

these changes by readjusting the flux of their Ca^{2+} and Cl^- channels to regain the turgor pressure. The readjustment also includes synthesis of new enzymes and intracellular relocalizations especially for the support and synthesis of cellular lipids against the shrinkage (Kirst, 1990).

The effect of shaking on microalgae was studied before as well. A study in 2012 showed that still *Chlorococcum spp.* cultures cultivated on 3N-BBM+V or BG-11 had a higher value of lipid accumulation than shaking cultures. On the other hand, shaking cultures had a higher amount of chlorophyll, carbohydrate and protein content than still cultures (Kirrolia et al., 2012).

1.7 *Parachlorella kessleri*

Microalgae can produce many different kinds of lipids, hydrocarbons and other complex oils (Singh et al., 2011) but only a limited number of algal oils are suitable for biodiesel production. For example, storage lipids (TAGs) accumulating microalgae species are very convenient for biofuel production. *Chlorella*, which is one of the members of trebouxiophycean genera, has been studied before regarding its very high photosynthetic growth rate and excellent biomass productivity (Morita et al., 2000). The Trebouxiophyceae are a class of green algae, which contain *Chlorellales, Prasiolales and Trebouxiales* (Friedl, 1995).

Chlorella and the closely related genus *Parachlorella* are the producers of triacylglycerols (TAGs) and long chain fatty acids for biodiesel production (Fernandes et al., 2013). A unicellular green alga *Parachlorella kessleri* is capable of reaching a very high biomass, starch, and lipid productivity levels without adhering to

bioreactor surfaces and forming aggregates (Ota et al., 2016). In addition, it is tolerant to high temperatures and resistant to shear stress (Fernandes et al., 2013).

1.7.1 *Parachlorella kessleri* genome

Ota et al. (2016) reported the sequence of the *Parachlorella kessleri* genome. 62.5 megabase pair (Mbp) length *Parachlorella kessleri* genome contains 13,057 identified genes. GC content is 58.30 %. There is a total of 400 scaffolds and the average scaffold size is 156,382 bp. 49.7 % of the proteins are associated with Kyoto encyclopedia of genes and genomes (KEGG) orthology numbers. Contig number is 5168 and the average contig size is 11,748 bp. The longest contig size is 198,966 bp. The average protein length is 467.0 aminoacids and the average gene density is 4.8 kb/gene. The average number of exons per gene is 7.9 exons. The average exon length is 176.3 bp. The average coding sequence is 29.30 %.

1.7.2 Growth conditions of *Parachlorella kessleri*

Parachlorella kessleri and many other algae synthesize fatty acids regarding the growth conditions. Under favorable growth conditions, synthesized fatty acids are mainly used for esterification into glycerol-based polar lipids. On the other hand, stress conditions cause algae to alter their biosynthetic pathways to form triacylglycerol (TAG) as a storage lipid (Breuer et al., 2012; Li et al., 2011). Microalgae lipid content can be increased by inducing nitrogen, iron, sulfur, phosphate deficiency and exposure to a high salt and iron concentrations (Fernandes et al. 2013; Li et al. 2013; Li et al. 2014; Minhas et al. 2016). Starch content can be also increased by nitrogen, sulfur depletion and a higher CO_2 concentration (Pribyl et

al. 2012; Li et al. 2013). However, growth rate and system productivity are negatively affected by such stress (Li et al., 2013).

Recent studies have elucidated some metabolic and transcriptomic responses of *Parachlorella kessleri* under stress conditions (Li et al., 2013). The elimination of nitrogen, sulfur or phosphorus causes an accumulation of lipids. Effect of sulfur elimination on lipid accumulation was less potent than the effect of nitrogen or phosphorus elimination. There is another undesirable effect of sulfur elimination. It progressively leads to cell death within cultivation time. *Parachlorella kessleri* cultures require aeration with 2% CO_2 for optimal growth. CO_2 limitation decreases the rate of lipid accumulation. The effect of nutrient depletion is stronger than the effect of CO_2 depletion, the total chlorophyll content decreases faster than it does under CO_2 limitation. Recent studies have also shown that the fatty acid composition of the cultures grown under different conditions differs each other. Under the optimal growth condition, the ratio of saturated, and unsaturated fatty acids is 0.917. Under nutrient limitation, the ratio of saturated, and unsaturated fatty acids is 0.55 (Li et al., 2013).

The type of cultivation is also important for the biomass productivity, specific growth rate, biomass yield and biomass doubling time. Among three different cultivation conditions: autotrophic, photoheterotrophic and mixotrophic, the mixotrophic cultivation with sufficient aeration conditions gave the best biomass yield of *Parachlorella kessleri*. In addition, daily oil, carbohydrate, and protein production was the highest under mixotrophic cultivation (Piasecka et al., 2017).

1.7.3 Mechanisms of Fatty Acids and Triacylglycerol biosynthesis in *Parachlorella kessleri* and other eukaryotic microalgae

Chloroplasts of green algae such as *Parachlorella kessleri*, *Chlorella vulgaris*, and *Chlamydomonas reinhardtii* are the center of fatty acid biosynthesis. Acetyl-CoA is converted into malonyl-CoA by acetyl-CoA carboxylase (*ACCase*) in the chloroplast. This step is the major rate limiting step. Next, malonyl-CoA is converted to malonyl-ACP by malonyl-CoA transacylase. Malonyl-ACP is converted to acyl-ACP by type II fatty acid synthase (Type II FAS). Acyl-ACP thioesterases (FAT) are responsible for the conversion of Acyl-ACP into free fatty acids (Lei et al. 2012; Hernandez-Torres et al. 2016). *accD* is one subunit of *ACCase* and it is encoded by the chloroplast genome of *P. kessleri* (Lu et al., 2012).

TAG synthesis occurs via two main pathways in eukaryotic microalgae; via an acyl-CoA independent pathway or the acyl-CoA dependent pathway (Kennedy pathway). The acyl-CoA dependent pathway occurs in endoplasmic reticulum and the acyl-CoA independent pathway occurs in the chloroplast. In the acyl-CoA independent pathway, acyl-ACP is incorporated into molecules of glycerol-3-phosphate by a glycerol-3-phosphate acyltransferase (GPAT), forming lysophosphatidate (LPA) by acylation. Next, lysophosphatidate (LPA) is converted into phosphatidate (PA) by lysophosphatidic acid acyltransferase (LPAT/LPAAT). Phosphatidic acid phosphatase (PAP) removes a phosphate group from phosphatidate (PA) and results in diacylglycerol (DAG) formation. Finally, diacylglycerol is converted into neutral TAGs and lipid droplets by diacylglycerol acyltransferase (DGAT) enzymes. In the Kennedy pathway, acyl-CoA molecules formed by long-chain acyl-CoA synthetase

from free fatty acids (FFAs) are incorporated into molecules of glycerol-3-phosphate by a glycerol-3-phosphate acyltransferase (GPAT), forming lysophosphatidate (LPA) by acylation. Next, lysophosphatidate (LPA) is converted into phosphatidate (PA) by lysophosphatidic acid acyltransferase (LPAT/LPAAT). Phosphatidic acid phosphatase (PAP) removes a phosphate group from phosphatidate (PA) and result in diacylglycerol (DAG) formation. Finally, diacylglycerol is converted into neutral TAGs and lipid droplets by diacylglycerol acyltransferase (DGAT) enzymes (Garay et al. 2014; Li et al. 2014).

1.7.4 Carbon fixation in *Parachlorella kessleri*

Ribulose-1,5-bisphosphate carboxylase/oxygenase (RuBisCO) is one of the major enzymes that function in the first major step of carbon fixation. Carbon fixation is the first phase of Calvin cycle and it is very important for photosynthetic organisms to convert atmospheric carbon dioxide into energy-rich molecules such as glucose. The Calvin cycle consists of three phased redox reactions occur in the stroma of chloroplast in photosynthetic organisms. In phase I, ribulose 5 phosphate is converted to ribulose-1,5-bisphosphate (RuBP). After that, ribulose-1,5-bisphosphate (RuBP) is carboxylated by ribulose-1,5-bisphosphate carboxylase (RuBisCO) with CO_2 and 3-phosphoglycerate is produced. In phase II, one molecule of 3-phosphoglycerate is converted to 1,3-bisphosphoglycerate and reduced to glyceraldehyde-3-phosphate. The other molecule of 3-phosphoglycerate leaves the cycle to be reduced to glyceraldehyde 3-phosphate (G3P). In phase III, glyceraldehyde-3-phosphate is converted to ribulose 5 phosphate to regenerate the ribulose. In *Parachlorella kessleri* and many other phototrophic organisms, RuBisCO consists of the large and small

chain. Large chain is about 55,000 Da and the small chain is about 13,000 Da. The chloroplast DNA encodes the large-chain gene (*rbcL*) (Read and Tabita, 1994).

2. Aims and Objectives

The overall aim of this study was to investigate how media salinity and shaking effect influence the growth rate, lipid accumulation and the expression of the genes *accD* and *rbcL* in microalgae *Parachlorella kessleri*. To achieve this, I aimed to compare the growth of still and shaking algal cultures cultivated on 3N-BBM+V in different salinity by chlorophyll and turbidity assay, amplify the *accD* and *rbcL* genes and determine their expression levels using RT-qPCR. In the next step, measure, visualize, quantify and characterize the lipid content of *Parachlorella kessleri* using the fluorescent Nile red and thin layer chromatography.

3. Materials and Methods

3.1 3N-BBM+V Preparation

Stock solutions of each element were prepared individually according to the CCAP instructions. Compositions of stock solutions except for NaCl are given in Appendix 1. After dissolving 1 g of vitamin B_{12} in 1000 ml distilled water, 5 ml of B_{12} solution was taken from the solution and added to 495 ml of distilled water. Next, 4 different NaCl stock solutions were prepared according to Table 1. The molarity of NaCl solutions was 0.043 M, 1.5 M, 3.0 M and 4.0 M respectively.

Table 1: Composition of NaCl stock solutions

Stock Solutions	Added amount of NaCl in 1000 ml water	Last Concentration
Stock 1	2.5 g	0.043 M
Stock 2	88.0 g	1.5 M
Stock 3	175.0 g	3.0 M
Stock 4	233.0 g	4.0 M

In order to prepare final 3N-BBM+V medium in different salinities, NaCl and stock solutions of $NaNO_3$, $CaCl_2.2H_2O$, $MgSO_4.7H_2O$, $K_2HPO_4.3H_2O$, KH_2PO_4, trace element solution, vitamin B_1 and B_{12} were mixed according to the CCAP instructions. The salinity level of final 3N-BBM+V solutions were 4×10^{-4} M, 15×10^{-1} M, 3×10^{-1} M and 6×10^{-1} M respectively. 4×10^{-4} M is the standard salinity level of 3N-BBM+V. 6×10^{-1} M is the salinity level of seawater. For each medium, the amount of ingredients in Table 2 was used as default. At the end, final volumes were completed to 1 L by adding NaCl stock solutions and dH_2O displayed in Table 3. Filter sterilized Vitamin B_1 and B_{12} solutions were added to the medium after allowing media to be autoclaved and cool down to 23 °C. The average pH of final 3N-BBM+V was 6.7 ± 0.1.

Table 2: Default composition of final 3N-BBM+V

Stock Solutions	Added amount in 1000 ml water
NaNO3	30.0 ml
CaCl2.2H2O	10.0 ml
MgSO4.7H2O	10.0 ml
K2HPO4.3H2O	10.0 ml
KH2PO4	10.0 ml
Trace element solution	6.0 ml
Vitamin B1	1.0 ml
Vitamin B12	1.0 ml

Table 3: Modified composition of final 3N-BBM+V

No Salt	**Added amount in 1000 ml water**
NaCl Stock 1	10.0 ml
dH20	912.0 ml
Low Salt	**Added amount in 1000 ml water**
NaCl Stock 2	100.0 ml
dH20	822.0 ml
Medium Salt	**Added amount in 1000 ml water**
NaCl Stock 3	100.0 ml
dH20	822.0 ml
High Salt	**Added amount in 1000 ml water**
NaCl Stock 4	150.0 ml
dH20	772.0 ml

3.2 Inoculation and culturing

Before the inoculation, optical density and chlorophyll a, b content of 1:10 diluted *P. kessleri* stock culture were measured. The stock culture had grown under photoautotrophic conditions in the algal culture room. Algal culture room has 1000 Lx average intensity of white fluorescent light. Light/dark cycle is 16/8 hours and the temperature is 15°C ± 3°C. Eight experimental 3N-BBM+V cultures were prepared by inoculating 1 ml of 1:10 diluted *P. Kessleri* culture into 20 ml medium (Table 4). In addition, four more experimental cultures were prepared by inoculating 8 ml of 1:10 diluted *P. Kessleri* culture into 100 ml 3N-BBM+V in order to examine the effect of shaking on microalgae growth (Table 5). After the inoculation, the growth cultures were sent to the algae growth room to be grown for 5 weeks. Cultures 11 and 12 were grown on rotary at 100 rpm.

Table 4: Composition of experimental 3N-BBM+V cultures

Culture	MBBM	1:10 diluted stock	Salinity	Growth place
Culture 1	20 mL	1 mL	0.0004 M	Algae growth room-still
Culture 2	20 mL	1 mL	0.0004 M	Algae growth room-still
Culture 3	20 mL	1 mL	0.15 M	Algae growth room-still
Culture 4	20 mL	1 mL	0.15 M	Algae growth room-still
Culture 5	20 mL	1 mL	0.3 M	Algae growth room-still
Culture 6	20 mL	1 mL	0.3 M	Algae growth room-still
Culture 7	20 mL	1 mL	0.6 M	Algae growth room-still
Culture 8	20 mL	1 mL	0.6 M	Algae growth room-still

Table 5: Composition of experimental 3N-BBM+V cultures

Culture	MBBM	1:10 diluted stock	Salinity	Growth place
Culture 9	100 mL	8 mL	0.0004 M	Algae growth room-still
Culture 10	100 mL	8 mL	0.0004 M	Algae growth room-still
Culture 11	100 mL	8 mL	0.0004 M	Algae growth room-shaker
Culture 12	100 mL	8 mL	0.0004 M	Algae growth room-shaker

Following 5 week of culturing 12 *Parachlorella kessleri* samples, a new experiment was set in order to see the growth dynamics of shaking *Parachlorella kessleri* cultures in different salinity. Before the inoculation, optical density and chlorophyll a, b content of 1:10 diluted *P. Kessleri* stock culture was measured. 6 experimental 3N-BBM+V cultures were prepared by inoculating 4 ml of 1:10 diluted *P. Kessleri* culture into 50 ml 3N-BBM+V. The NaCl molarity of the samples was; 4×10^{-4} M, 15×10^{-1} M and 3×10^{-1} M respectively. After the inoculation, the cultures were sent to algae growth room. All cultures were kept on rotary at 100 rpm for 5 weeks. The detailed compositions of 6 experimental 3N-BBM+V cultures are given in Table 6.

Table 6: Composition of experimental 3N-BBM+V cultures

Culture	MBBM	1:10 diluted stock	Salinity	Growth place
Culture 1	50 mL	4 mL	0.0004 M	Algae growth room-shaker
Culture 2	50 mL	4 mL	0.0004 M	Algae growth room-shaker
Culture 3	50 mL	4 mL	0.15 M	Algae growth room-shaker
Culture 4	50 mL	4 mL	0.15 M	Algae growth room-shaker
Culture 5	50 mL	4 mL	0.3 M	Algae growth room-shaker
Culture 6	50 mL	4 mL	0.3 M	Algae growth room-shaker

After 1 week of cultivation, 6 more *Parachlorella kessleri* samples were prepared in order to see the cell responses when they were transferred from the no salt to the high salt medium or from the medium salt to the no salt medium. 1 week grown cultures given in Table 6 were used as stock cultures. Before the inoculation, the optical density and chlorophyll a, b content of 1 week grown *P. Kessleri* cultures were measured. All of the cultures were started with the same chlorophyll concentration, 1.44 µg/mL. The final volumes were 50 mL. All cultures were stored on rotary at 100 rpm. The detailed composition of 6 experimental 3N-BBM+V cultures is given in Table 7. Culture 7 and 8 were inoculated with culture 1. Culture 9 and 10 were inoculated with culture 3. Culture 11 and 12 were inoculated with culture 6.

Table 7: Composition of experimental 3N-BBM+V cultures

Culture	MBBM	1:10 diluted stock	Stock Salinity	Medium Salinity	Growth place
Culture 7	4 mL	46 mL	0.0004 M	0.6 M	Algae growth room-shaker
Culture 8	4 mL	46 mL	0.0004 M	0.6 M	Algae growth room-shaker
Culture 9	6 mL	44 mL	0.15 M	0.6 M	Algae growth room-shaker
Culture 10	6 mL	44 mL	0.15 M	0.6 M	Algae growth room-shaker
Culture 11	7 mL	43 mL	0.3 M	0.0004 M	Algae growth room-shaker
Culture 12	7 mL	43 mL	0.3 M	0.0004 M	Algae growth room-shaker

3.3 Microscopic Examination

20 µL of cells were dropped onto a glass slide and covered with a glass slip. No air bubble was left when covering the sample. *P. kessleri* cells were examined and checked for contamination with a Leica DMR microscope by using 40x and 100x magnification.

3.4 Growth measurements

Algal growth was measured every seven days by measuring the absorbance of the 1 mL of each culture at 750 nm. For total chlorophyll analysis, 1 mL of algal culture was centrifuged at 14,000 *g* for 10 min. The supernatant was discarded and the pellet was resuspended in 1 mL of 100% methanol. The sample was placed on a hot block at 60° C for 25 min and centrifuged at 14,000 *g* for 10 min. Finally, the supernatant was transferred into a cuvette. The absorbance of the samples at 652 nm, 665 nm, and 750 nm was measured by Genesys 10S VIS spectrophotometer (ThermoFisher Scientific, Massachusetts, USA) and recorded. The total chlorophyll content (chlorophyll a and chlorophyll b) was calculated according to equation 1.

Equation 1: Chlorophyll a, b and total content formula by using absorbance (Ritchie, 2006).

$$\text{Chlorophyll a } (\mu g/mL) = (16.519 \times (A_{665} - A_{750})) - (8.0962 \times (A_{652} - A_{750}))$$

$$\text{Chlorophyll b } (\mu g/mL) = (-12.1688 \times (A_{665} - A_{750})) + (27.4405 \times (A_{652} - A_{750}))$$

$$\text{Total chlorophyll } (\mu g/mL) = \text{chlorophyll a} + \text{chlorophyll b}$$

3.5 Nile Red Staining and Lipid Analysis

Nile Red stock solution was prepared by dissolving 1 mg of Nile Red (Sigma N-3013) in 4 mL acetone. The solution was vortexed vigorously to dissolve the dye in the solvent. 4 µL of Nile Red stock solution was added to 1 mL, ½ diluted algal suspension. After vortexing, the tube was left for 10 min at room temperature. Stained cells were imaged by Leica DMR microscope using 3 different filter cubes; standard light, rhodamine light and fluorescein light. Table 8 displays the technical details of rhodamine and fluorescein filter cubes.

Table 8: Used range of Filter Cubes of Leica DMR microscope

Filter Cube	Excitation Range	Excitation Filter	Dichromatic Mirror	Suppression Filter
A (Fluorescein)	UV	BP 340-380	400	LP 425
N2.1 (Rhodamine)	Green	BP 515-560	580	LP 590

3.6 Gene selection and primer design

accD and *rbcL* genes were selected for this experiment because they have a very active role in the rate limiting steps of fatty acid and triacylglycerol metabolism of *Parachlorella kessleri* and other green microalgae (see sections 1.5.3, 1.5.4). The *18S rRNA* gene was selected as an internal reference in RT-qPCR. *Parachlorella kessleri accD*, *rbcL*, and *18S rRNA* coding sequences were available on National Center for Biotechnology Information database. The *rbcL*, and *18S rRNA* primers were designed by Chris McCusker and the *accD* primers were designed by myself in primer 3 software (Table 9).

Table 9: Selected primers for the *accD*, *rbcL*, and *18S rRNA* genes

Gene	Orientation	Sequence	Tm (°C)	Product size
18S rRNA	Forward	GTTTCTTCGATGACTCCGCC	59	223
	Reverse	TGCACCACCACCCATAGAAT	59	
rbcL	Forward	CACATGCCTGCTCTTGTTGA	58.76	167
	Reverse	CCTTCACGAGCAAGATCACG	59.01	
accD	Forward	GAATATGCCACTCAAGAAGG	54.87	198
	Reverse	AGCAAAGCTTGCTGTTACAC	55.88	

3.7 RNA extraction

RNA was extracted from *P. kessleri* cells using TriSure™ reagent (Bioline). 30 mL of each culture was centrifuged at 12,000 *g* for 2 min in order to obtain the pellet. The supernatant was discarded and the cells were homogenized in 1 mL of TriSure™ reagent by using acid washed <106 µm glass beads (Sigma) for 40 s in FastPrep FP120 tissue lyser (ThermoFisher Scientific, Massachusetts, USA). Following the the manufacturer's procedure, the pellet was air dried and dissolved in 50 µL of DEPC treated water. RNA concentrations were measured using NanoDrop Lite 2000c Spectrophotometer (ThermoFisher Scientific, Massachusetts, USA). RNA samples were stored at -80 ° C.

3.8 Lithium Chloride RNA Cleanup

4 M LiCI was prepared by dissolving 25.4 g LiCI in 250 mL DEPC treated water. 3 M sodium acetate ($NaOAc\text{-}3H_2O$) was prepared by dissolving 81.6 g $NaOAc\text{-}3H_2O$ in 200mL DEPC treated water. 30 µL 4 M LiCI solution was added to each of 30 µL RNA extract and placed on ice for 1 hour. Following the centrifugation at 12,000 *g* for 10 min, the supernatant was discarded and each pellet was resuspended in 100 µL DEPC treated water. In order to precipitate the RNA, 30 µL $NaOAc\text{-}3H_2O$ and 250 µL 95% EtOH were added. Each tube was centrifuged at 12,000 *g* for 10 min.

Following the removal of the supernatant, each pellet was suspended in 20 µL DEPC treated water (The Springer Lab, 2015)

3.9 cDNA synthesis

Quantified RNA samples were converted to cDNA by Tetro cDNA Synthesis Kit (Bioline). The final reaction volume was set to 20 µL; 10 µL extracted RNA, 1 µL Oligo $(dT)_{18}$, 1 µL dNTP mix (10 mM), 4 µL 5x RT Buffer, 1 µL Ribosafe RNase Inhibitor, 1 µL Tetro Reverse Transcriptase (200 u/ µL) and 2 µL DEPC-treated water. Following vortexing, the reaction mix was incubated at 45°C for 30 min and 85°C for 5 min respectively in Artik thermocycler (ThermoFisher Scientific, Massachusetts, USA). cDNA concentrations were measured using NanoDrop Lite 2000c Spectrophotometer (ThermoFisher Scientific, Massachusetts, USA). cDNA samples were stored at -20 ° C.

3.10 End Point PCR

End point PCR used to check the DNA quality and the primer specificity of the *Parachlorella kessleri* genes: *accD*, *rbcL* and *18S rRNA*. For each reaction, final reaction volume was set to 50 µL: 2 µL cDNA, 1 µL gene specific reverse and forward primers (20 µM each), 25 µL 2x MyFi Mix and 21 µL ddH_2O. The reaction was done in an Artik thermocycler (Thermofisher, Massachusetts, USA). PCR cycling conditions were as follows: 1 min at 95 °C for initial denaturation, followed by 30 cycles of 30 s at 95 °C for denaturation, 30 s at 55 °C for annealing and 30 s at 72 ° C for extension. At the end of 30 cycles, samples were held at 72 ° C for 1 min followed by 4 °C final temperature. The amplified products were run on 1% agarose gel for 30 min at 100V and visualized by Gel Doc™ EZ Imager (BIO-RAD).

3.11 Real-time quantitative PCR

Real time quantitative PCR was used for the quantification of the expression level of the *accD* and *rbcL* genes of *Parachlorella kessleri*. The final reaction volume was set to 20 µL: 5 µL cDNA, 0.8 µL gene specific reverse and forward primers (10 µM each), 10 µL 2x SensiFAST SYBR® No-Rox MixMyFi Mix and 3.4 µL ddH_2O. The reaction was done in CFX Connect qPCR machine (BioRad, Berkeley, USA). Real time PCR cycling conditions were as follows: 1 min at 95 °C for initial denaturation, followed by 40 cycles of 5 s at 95 °C for denaturation, 10 s at 60 °C for annealing and 10 s at 72 °C for extension. Comparative C_T method was used to determine the relative fold expression of the genes *accD* and *rbcL*. First of all, average C_T value of each gene was analyzed. Secondly, the difference in C_T between 18s rRNA reference sequence and each gene was calculated (ΔCT). Finally, the relative fold difference in expression of each gene was calculated by subtracting the difference in expression of the target gene from the difference in expression of the reference gene (Schmittgen and Livak, 2008).

3.12 Lipid Extraction

Algal lipids were extracted by Folch Method (Folch et al., 1957). 30 ml of each algal sample was put into a 50 ml Falcon tube and centrifuged at 4,000 *g* for 10 min (Eppendorf Centrifuge 5810, Germany). Discarding the supernatant and weighting the pellet, x 20 volume of the pellet of 2:1 chloroform-Methanol solution was added. Each mixture was vortexed and agitated in an orbital shaker for 30 min. Following centrifugation at 4,000 *g* for 10 min, the upper liquid phase was transferred to another tube and washed with 0.2 volume of 0.9% NaCl. Each mixture was vortexed and centrifuged at 2,000 *g* for 5 min. Following the removal of the upper phase and

interphase by pipetting, the volume of the lower chloroform phase was decreased to 0.1 mL by passing through nitrogen streaming.

3.13 Thin Layer Chromatography (TLC)

10 µL of each algal lipid sample, 2 µL of sunflower seed oil, 2 µL of 1:10, 1:20, 1:30, 1:40, 1:50 and 1:100 diluted sunflower seed oil were loaded on TLC plates. As mobile phase solvent, hexane, diethyl ether, acetic acid (85: 15: 1) was used. Keeping the 75 mL of solvent in the glass tank for 30 min for the equilibration, the plate was placed inside the glass tank until the solvent reached 1 cm away from the top of the plate. Following air dry, the plate was dipped into 5% molybdophosphoric acid for 5 seconds and placed in an oven at 100 °C for 15 min (Mannikin et al., 1984). The Rf values were calculated according to the formula below;

$$Rf = \frac{\text{Distance moved by the solute}}{\text{Distance from pigment origin to solvent front}}$$

3.14 Phylogenetic Analysis of the *rbcL* and *accD* genes

Amino acid sequences of the *rbcL* and *accD* proteins of *P. kessleri* were taken from the protein data bank. FASTA sequences of the proteins were submitted to the blastp at the National Centre for Biotechnology Information (NCBI) to obtain amino acid sequences producing significant alignments with the *rbcL* and *accD* sequences of *Parachlorella kessleri*. The sequences were selected regarding their sequence identity. For each protein, 9 sequences from different organisms were selected according to their sequence homology. Selected sequences were submitted to the phylogeny.fr. The phylogenetic tree was constructed automatically.

4. Results

4.1 Growth analysis of algal cultures cultivated on the bold basal media in different salinity

In all samples, there was a strong positive correlation between mean total chlorophyll and optical density at 750 nm. Among the still cultures in different salinity, algal cultures cultivated on no salt 3N-BBM+V had the highest growth rate. Algal cultures on low salt 3N-BBM+V had the second highest growth rate, but the rise in growth started to drop eminently after day 28. Algal cultures on medium salt 3N-BBM+V had the third highest growth rate. As the salinity of the medium increases, the start of the rapid growth was delayed. Cells cultivated on no salt 3N-BBM+V started the rapid growth around day 15. Cells cultivated on low salt 3N-BBM+V started the rapid growth around day 20. Cells cultivated on medium salt 3N-BBM+V started the rapid growth around day 30. Cells cultivated on high salt 3N-BBM+V could not start the rapid growth at the end of day 35.

A

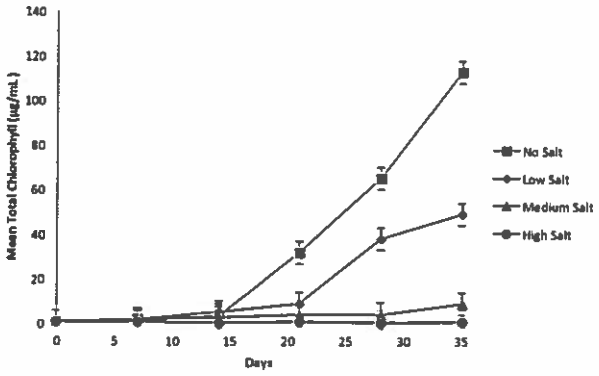

B

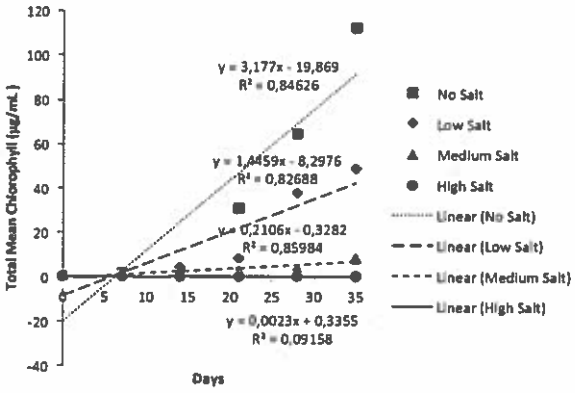
y = 3,177x - 19,869
R² = 0,84626
y = 1,4459x - 8,2976
R² = 0,82688
y = 0,2106x - 0,3282
R² = 0,85984
y = 0,0023x + 0,3355
R² = 0,09158
No Salt
Low Salt
Medium Salt
High Salt
Linear (No Salt)
Linear (Low Salt)
Linear (Medium Salt)
Linear (High Salt)
Total Mean Chlorophyll (µg/mL)
Days

C

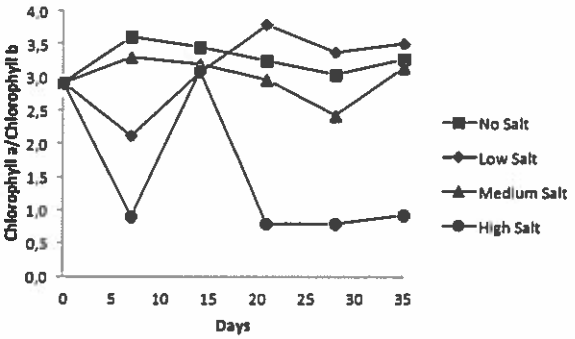
Chlorophyll a/Chlorophyll b
Days
No Salt
Low Salt
Medium Salt
High Salt

D

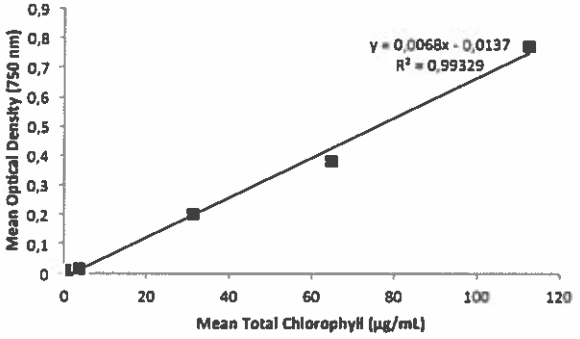
y = 0,0068x - 0,0137
R² = 0,99329
Mean Optical Density (750 nm)
Mean Total Chlorophyll (µg/mL)

E

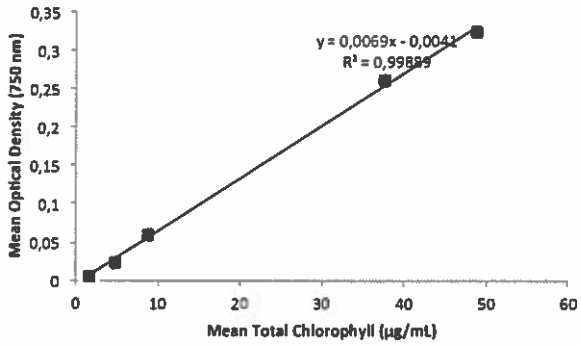

F

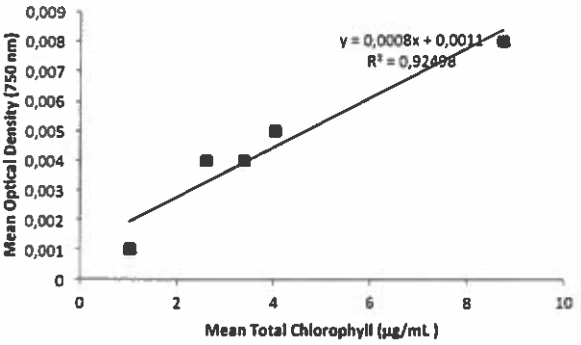

Figure 2: (A) Mean total chlorophyll (µg/mL) of *Parachlorella kessleri* cells cultivated on 3N-BBM+V in different salinity. The measurements were recorded once a week for 5 weeks. (B) Chlorophyll growth rate and R-square values of *Parachlorella kessleri* cells cultivated on bold basal media in different salinity for 5 weeks. In the y=mx+n formula, the slope m is the indicative of growth rate. R-square value shows the statistical closeness of the data to the regression line. (C) Mean chlorophyll a / chlorophyll b ratio of algal cells cultivated in different salinity. (D) The correlation between mean optical density (750 nm) and mean total chlorophyll (µg/mL) for *P. kessleri* grown on no salt 3N-BBM+V. (E) The correlation between mean optical density (750 nm) and mean total chlorophyll (µg/mL) for *P. kessleri* grown on low salt 3N-BBM+V. (F) The correlation between mean optical density (750 nm) and mean total chlorophyll (µg/mL) for *P. kessleri* grown on medium salt 3N-BBM+V.

4.2 Growth analysis of shaking and still algal cultures cultivated on the bold basal media

In both samples, there was a strong positive correlation between mean total chlorophyll and optical density at 750 nm. The shaking cultures displayed a higher growth rate than the still cultures. In contrast to the shaking cultures, the total chlorophyll content in the still cultures could not increase exponentially. At the end of week 5, the still cultures were almost in the stationary phase. On the other hand, shaking cells would need longer time to enter the stationary phase.

A

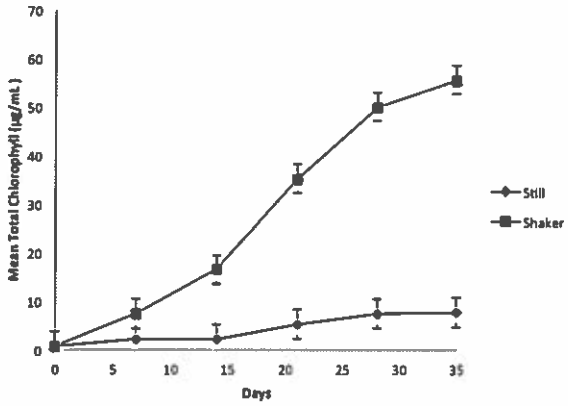

B

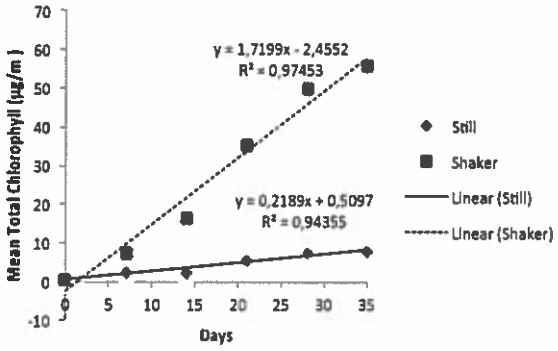

C

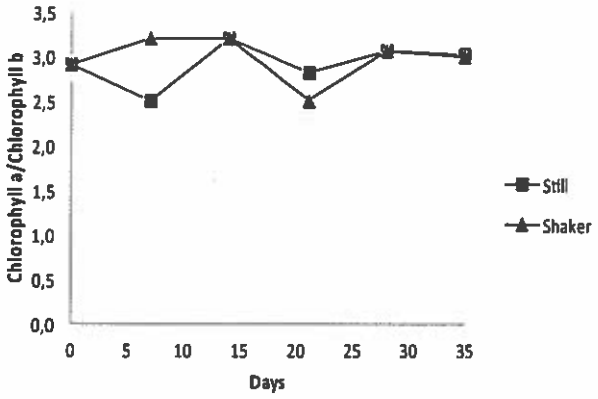

D

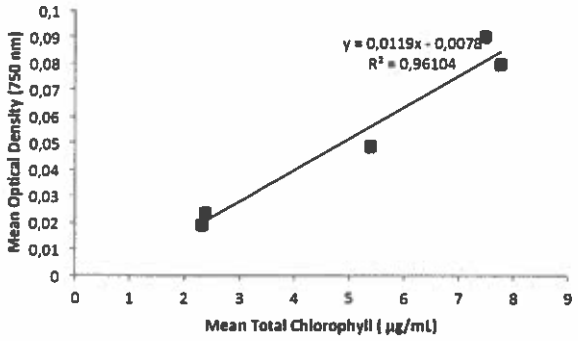

E

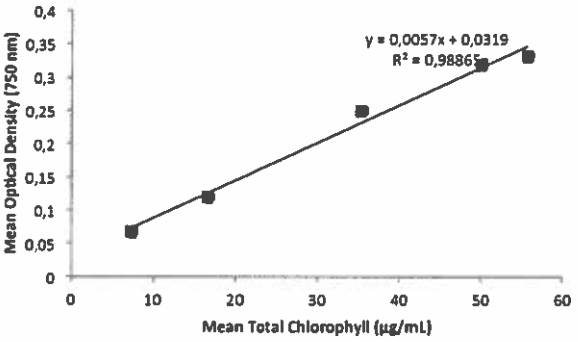

Figure 3: (A) Mean total chlorophyll (µg/mL) of *Parachlorella kessleri* cultivated on 3N-BBM+V in still or shaking environment. The measurements were recorded each

week for 5 weeks. (B) Growth rate and R-square values of *Parachlorella kessleri* cells cultivated on bold basal media in different salinity for 5 weeks. In the y=mx+n formula, the slope m is the indicative of growth rate. R-square value shows the statistical closeness of the data to the regression line. (C) Mean chlorophyll a / chlorophyll b ratio of shaking and still algae cultures. (D) The correlation between mean optical density (750 nm) and mean total chlorophyll (µg/mL) for still *P. kessleri* grown on 3N-BBM+V. (E) The correlation between mean optical density (750 nm) and mean total chlorophyll (µg/mL) for shaking *P. kessleri* grown on 3N-BBM+V.

4.3 Growth analysis of shaking algal cultures cultivated on the bold basal media in different salinity

In all samples, there was a strong positive correlation between mean total chlorophyll and optical density at 750 nm. No salt 3N-3N-BBM+V cultures had the highest growth rate. Low salt 3N-BBM+V cultures had the second highest growth rate, but the rise in their growth rate started to drop eminently after day 28. In all cultures, rapid growth was started around day 7. Still cultures on low salt 3N-BBM+V displayed a higher growth rate than shaking cultures on low salt 3N-BBM+V. In contrast, shaking cultures on medium salt 3N-BBM+V displayed a higher growth rate than still cultures on medium salt 3N-BBM+V.

A

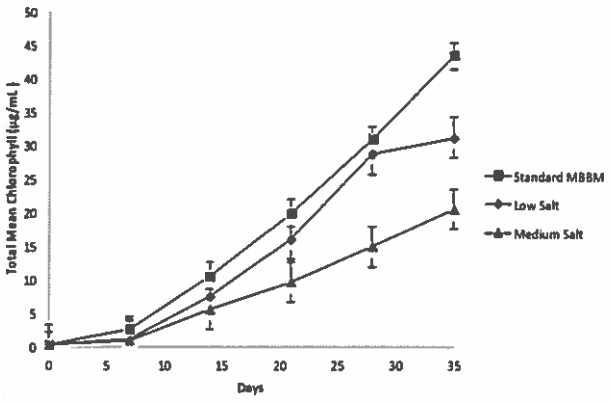

B

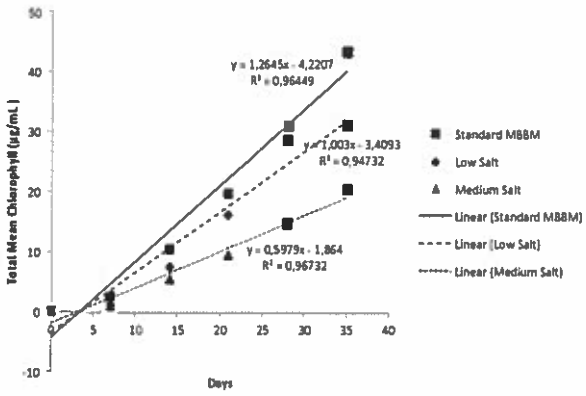
y = 1,2645x - 4,2207
R² = 0,96449
y = 1,003x - 3,4093
R² = 0,94732
y = 0,5979x - 1,864
R² = 0,96732
Total Mean Chlorophyll (µg/mL)
Days
Standard MBBM
Low Salt
Medium Salt
Linear (Standard MBBM)
Linear (Low Salt)
Linear (Medium Salt)

C

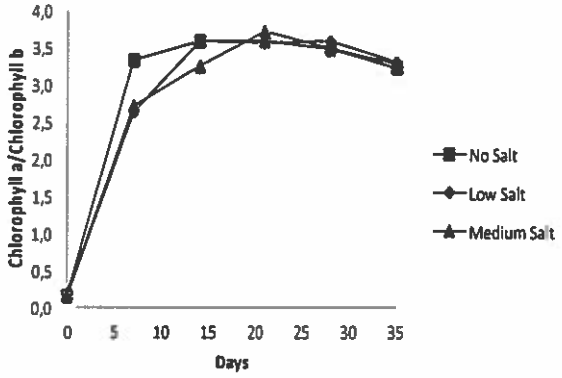
Chlorophyll a/Chlorophyll b
Days
No Salt
Low Salt
Medium Salt

D

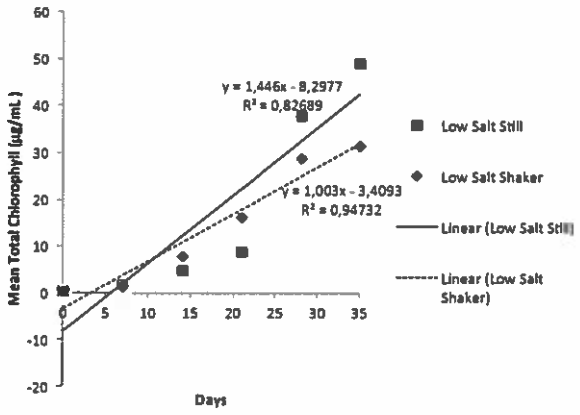
y = 1,446x - 8,2977
R² = 0,82689
y = 1,003x - 3,4093
R² = 0,94732
Mean Total Chlorophyll (µg/mL)
Days
Low Salt Still
Low Salt Shaker
Linear (Low Salt Still)
Linear (Low Salt Shaker)

E

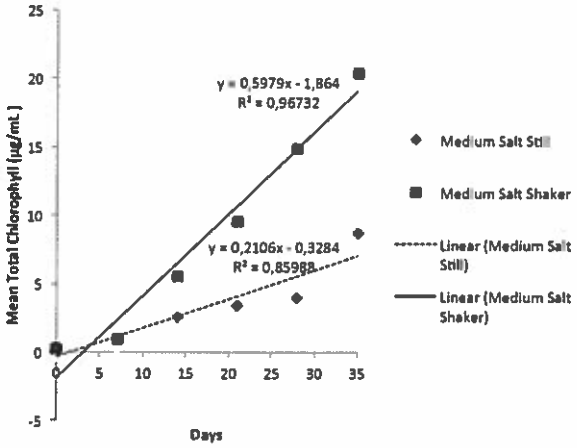
y = 0,5979x - 1,864
R² = 0,96732
y = 0,2106x - 0,3284
R² = 0,85988
Medium Salt Still
Medium Salt Shaker
Linear (Medium Salt Still)
Linear (Medium Salt Shaker)
Mean Total Chlorophyll (µg/mL)
Days

F

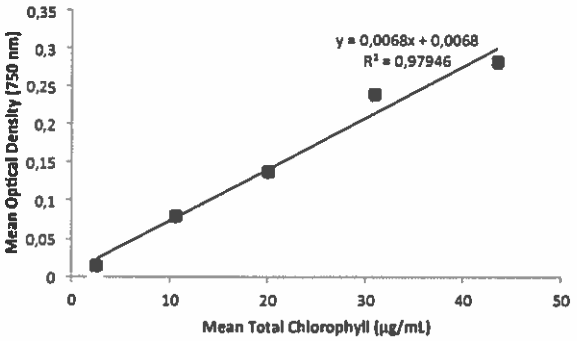
y = 0,0068x + 0,0068
R² = 0,97946
Mean Optical Density (750 nm)
Mean Total Chlorophyll (µg/mL)

G

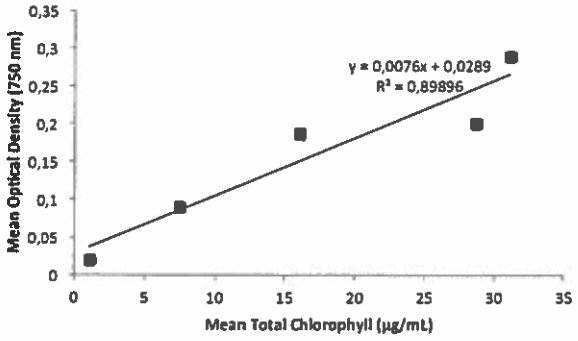
y = 0,0076x + 0,0289
R² = 0,89896
Mean Optical Density (750 nm)
Mean Total Chlorophyll (µg/mL)

H

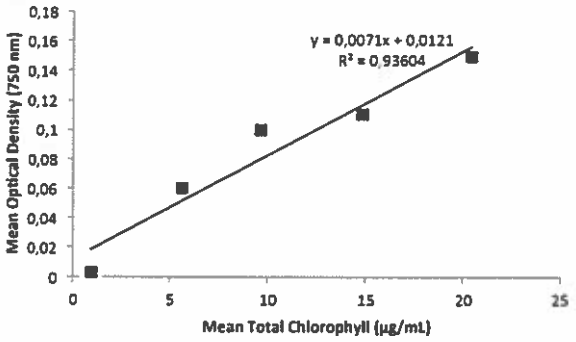

Figure 4: (A) Mean total chlorophyll (µg/mL) of shaking *Parachlorella kessleri* cells cultivated on 3N-BBM+V in different salinity. The measurements were recorded each week for 5 weeks. (B) Growth rate and R-square values of *Parachlorella kessleri* cells cultivated on bold basal media in different salinity on rotary for 5 weeks. In the y=mx+n formula, the slope m is the indicative of growth rate. R-square value shows the statistical closeness of the data to the regression line. (C) Mean chlorophyll a / chlorophyll b ratio of algal cells. (D) Total chlorophyll growth rate and R-square values of *Parachlorella kessleri* cells cultivated on low salt bold basal media on rotary or still for 5 weeks. (E) Total chlorophyll growth rate and R-square values of still and shaking *Parachlorella kessleri* cells cultivated on medium salt bold basal media for 5 weeks. (F) The correlation between mean optical density (750 nm) and mean total chlorophyll (µg/mL) for shaking *P. kessleri* grown on no salt 3N-BBM+V. (G) The correlation between mean optical density (750 nm) and mean total chlorophyll (µg/mL) for shaking *P. kessleri* grown on low salt 3N-BBM+V. (H) The correlation between mean optical density (750 nm) and mean total chlorophyll (µg/mL) for shaking *P. kessleri* grown on medium salt 3N-BBM+V.

4.4 Growth analysis of algal cultures transferred from the no salt to the high salt, low salt to the high salt and high salt to the no salt 3N-BBM+V

The growth rate of the cells transferred from high salt 3N-BBM+V to no salt 3N-BBM+V were very similar to the growth rate of the cells just grown on no salt 3N-BBM+V. On the other hand, neither the cells transferred from low salt 3N-BBM+V to high salt 3N-BBM+V nor the cells transferred from the no salt 3N-BBM+V to the high salt 3N-BBM+V were able to grow.

A

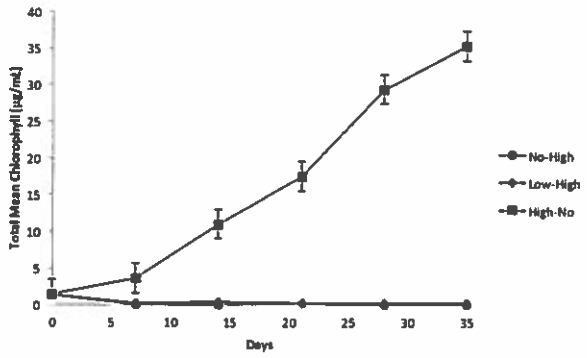

B

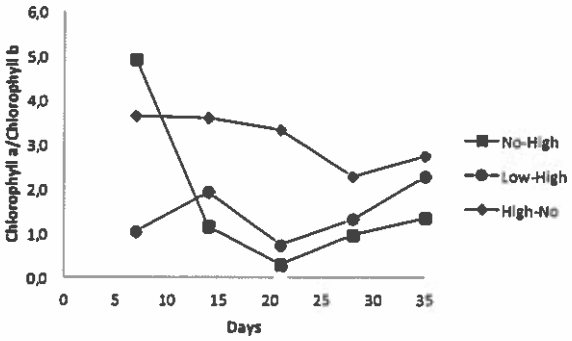

Figure 5: (A) Mean total chlorophyll (µg/mL) of *Parachlorella kessleri* cells transferred from the no salt to the high salt, low salt to the high salt and high salt to the no salt basal media. The measurements were recorded once a week for 5 weeks. (B) Mean estimated chlorophyll a / chlorophyll b ratio of algal cells.

4.5 Gene characterization of *Parachlorella kessleri* cells

Expected amplicon sizes of *18S rRNA*, *rbcL* and *accD* were 223 bp, 167 bp, and 198 bp respectively. The expected sizes were compatible with the band sizes on the gel (Figure 3). No unspecific product was detected.

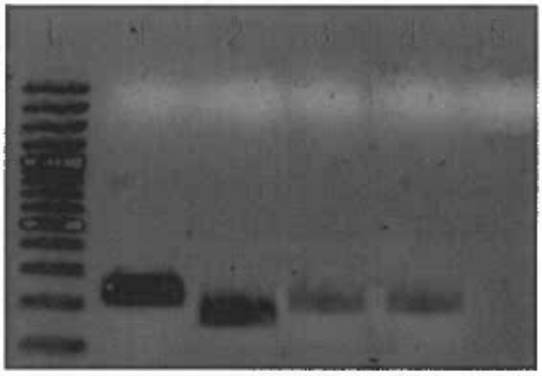

Figure 1: End point PCR products of cells cultivated on no salt still cultures run on 1% agarose gel. Following RNA extraction, cDNA synthesis and end point PCR amplification with the specific primers in Table 9, Samples were run at 100 V for 30 min. (L) GeneRuler 100 bp Plus DNA Ladder (Thermo Scientific). (1) *18S rRNA*. (2) *rbcL*. (3,4) *accD* from the same source. (5) Negative Control.

4.6 The fold expression analysis of the accD and rbcL genes of algal cells grown on the still bold basal media in different salinity

RT-qPCR analysis indicated 2.6 fold higher expression of the *accD* gene and 4 fold higher expression of the *rbcL* gene of low salt still 3N-BBM+V culture compared to no salt still 3N-BBM+V culture. Relative expression of the *accD* gene of no salt still 3N-BBM+V culture was 3.4 fold higher compared to medium salt still 3N-BBM+V culture. Relative expression of the *accD* gene of no salt still 3N-BBM+V culture was 2.7 fold higher compared to high salt still 3N-BBM+V culture.

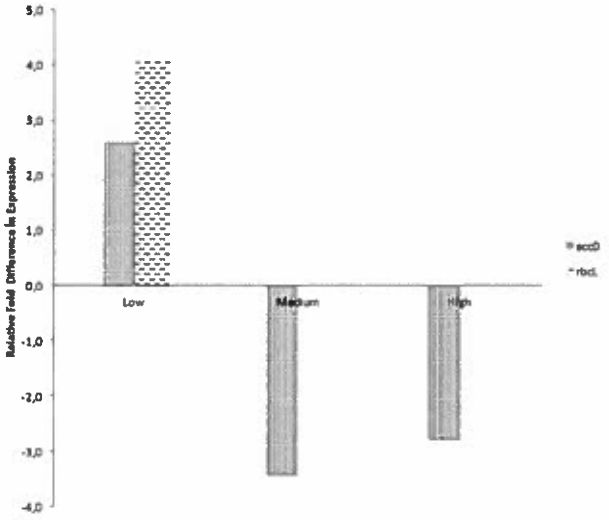

Figure 6: The relative fold differences in expression of the *accD* and *rbcL* genes of algal cells cultivated on low salt (0.15 M), medium salt (0.3 M) and high salt (0.6 M) media (Comparative C_T method). Expression profile of algal cells cultivated on the no salt 3N-BBM+V was used as the reference. 18s RNA gene was used as the reference gene. The fold differences in expressions were calculated regarding the RT-qPCR data. The relative fold differences below the value of 2 were discarded.

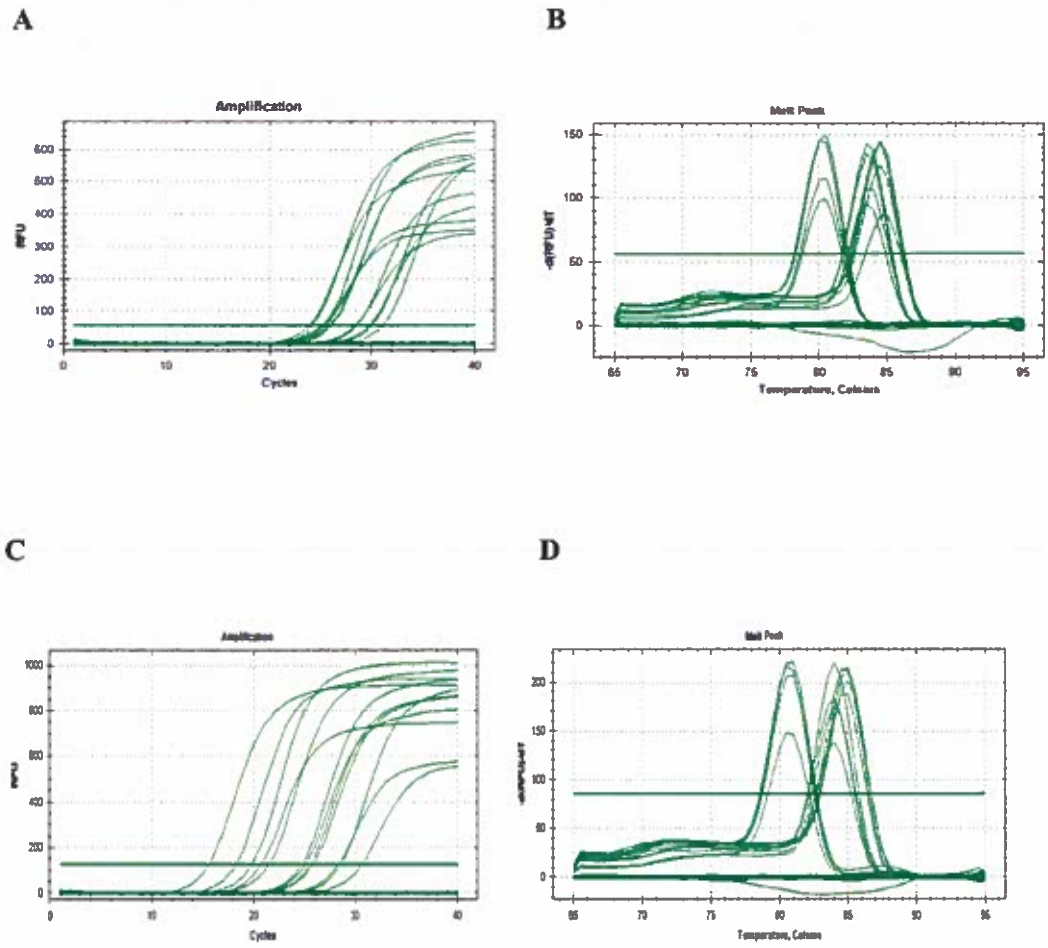

Figure 7: (A) Real time amplification curves of the *18s rRNA*, *rbcL* and *accD* transcripts of algal cells cultivated on no salt and low salt media. (B) Melt peak curves of the *18s rRNA*, *rbcL* and *accD* transcripts of algal cells cultivated on no salt and low salt media. (C) Real time amplification curves of the *18s rRNA*, *rbcL* and *accD* transcripts of algal cells cultivated on medium salt and high salt media. (D) Melt peak curves of the *18s rRNA*, *rbcL* and *accD* transcripts of algal cells cultivated on medium salt and high salt media. The negative control was used for each primer set to check contamination.

4.7 The fold expression analysis of the accD and rbcL genes of shaking and still algal cultures cultivated on the bold basal media

After RT-qPCR study of the *accD* and *rbcL* genes of shaking and still algal cells, it was inferred that the relative fold difference in expression of the *accD* and *rbcL* genes between the shaking and still algal cultures were below the value of 2; thus they were considered as insignificant.

A B

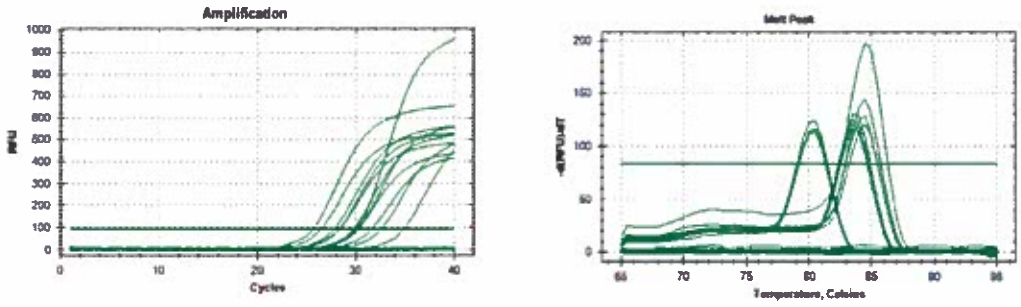

Figure 8: (A) Real time amplification curves of the *18s rRNA*, *rbcL* and *accD* transcripts of shaking and still algal cells. (B) Melt peak curves of the *18s rRNA*, *rbcL* and *accD* transcripts of shaking and still algal cells. The negative control was used for each primer set to check contamination.

4.8 The fold expression analysis of the *accD* and *rbcL* genes of shaking algal cells cultivated on bold basal media in different salinity

When cultures in different salinity were cultivated on rotary, relative expression of the *accD* and *rbcL* genes of no salt shaking 3N-BBM+V culture was 7.4 fold higher compared to low salt shaking 3N-BBM+V culture. In contrast, medium salt shaking 3N-BBM+V culture displayed 2.7 fold higher expression of the *accD* gene and 3.8 fold higher expression of the *rbcL* gene compared to no salt shaking 3N-BBM+V culture.

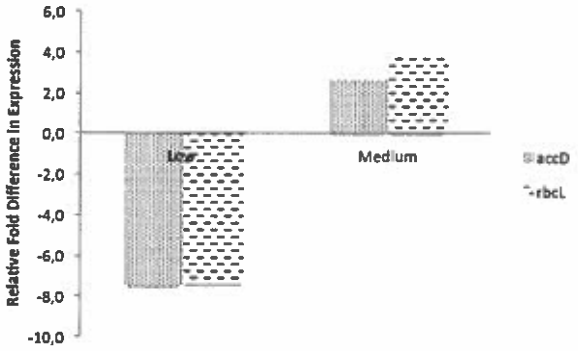

Figure 9: The relative fold differences in expression of the *accD* and *rbcL* genes of algal cells cultivated on bold basal media in different salinity (Comparative C_T method). Expression profile of algal cells cultivated on no salt 3N-BBM+V was used as the reference. The *18s rRNA* gene was used as the reference gene. The fold difference in expressions were calculated regarding the RT-qPCR data.

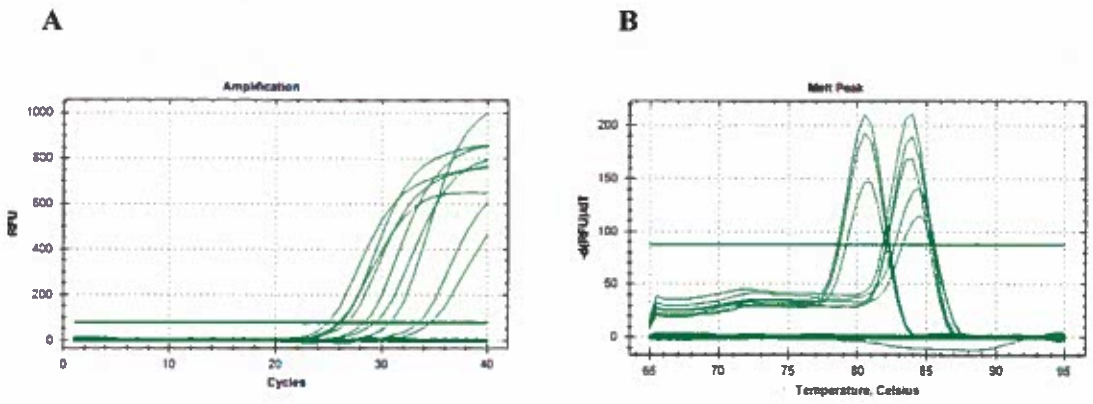

Figure 10: (A) Real time amplification curves of *18s rRNA*, *rbcL* and *accD* transcripts of shaking algal cultures cultivated on no salt, low salt, and medium salt 3N-BBM+V. (B) Melt peak curves of *18s rRNA*, *rbcL* and *accD* transcripts of shaking algal cultures cultivated on no salt, low salt, and medium salt 3N-BBM+V. The negative control was used for each primer set to check contamination.

4.9 The fold expression analysis of the accD and rbcL genes of algal cultures transferred from no salt to high salt, low salt to the high salt and high salt to no salt 3N-BBM+V

RT-qPCR analysis indicated that cells transferred from high salt to no salt 3N-BBM+V had 2 fold higher expression of the *accD* and *rbcL* genes compared to the cells transferred from low salt to high salt 3N-BBM+V. There was no significant fold difference in expression of the *accD* and *rbcL* genes between algal cells transferred from the no salt to the high salt and the algal cells transferred from the high salt to the no salt 3N-BBM+V. In addition, there was no significant fold difference in expression of the *accD* and *rbcL* genes between algal cells transferred from the no salt to the high salt and algal cells transferred from the low salt to the high salt 3N-BBM+V.

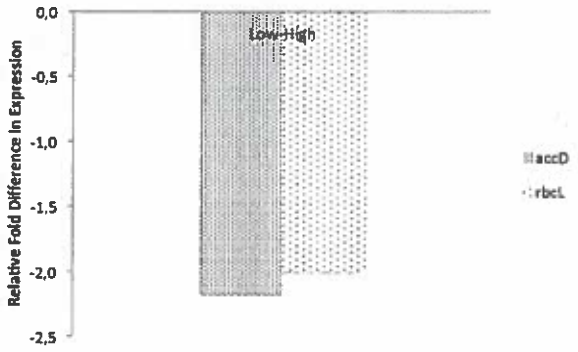

Figure 11: The relative fold differences in expression of the *accD* and *rbcL* genes of algal cells transferred from the low salt to the high salt compared with the algal cells transferred from the high salt to the no salt (Comparative C_T method). Expression profile of algal cells transferred from the high salt to the no salt 3N-BBM+V was used as the reference. The *18s rRNA* gene was used as the reference gene. The fold differences in expressions were calculated regarding the RT-qPCR data. The relative fold differences below the value of 2 were discarded.

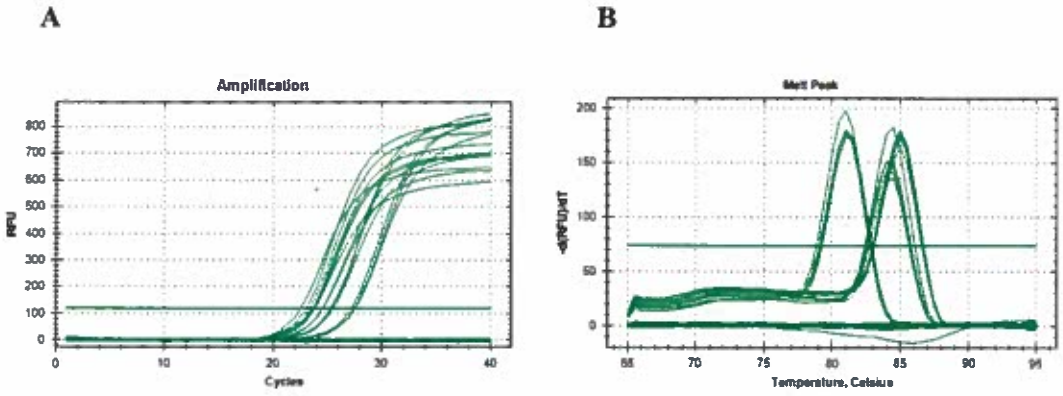

Figure 12: (A) Real time amplification curves of the *18s rRNA*, *rbcL* and *accD* transcripts of algal cultures transferred from the no salt to the high salt, low salt to the high salt and high salt to the no salt 3N-BBM+V. (B) Melt peak curves of the *18s rRNA*, *rbcL* and *accD* transcripts of algal cultures transferred from the no salt to the high salt, low salt to the high salt and high salt to the no salt 3N-BBM+V. The negative control was used for each primer set to check contamination.

4.10 Microscopic analysis of *Parachlorella kessleri*

Chlorophyll content and circular shape of 25-day old cells were imaged by both 40x and 100x magnification. The average diameter of the cells was between 3-6 μm. It was observed that some cells were attached each other. In addition, bundle formation was detected. Green chlorophyll content was visible in both images. Nuclei of the cells were seen as pale spots. The reason of the colour difference is due to the lack of chlorophyll content in the nucleus.

A B

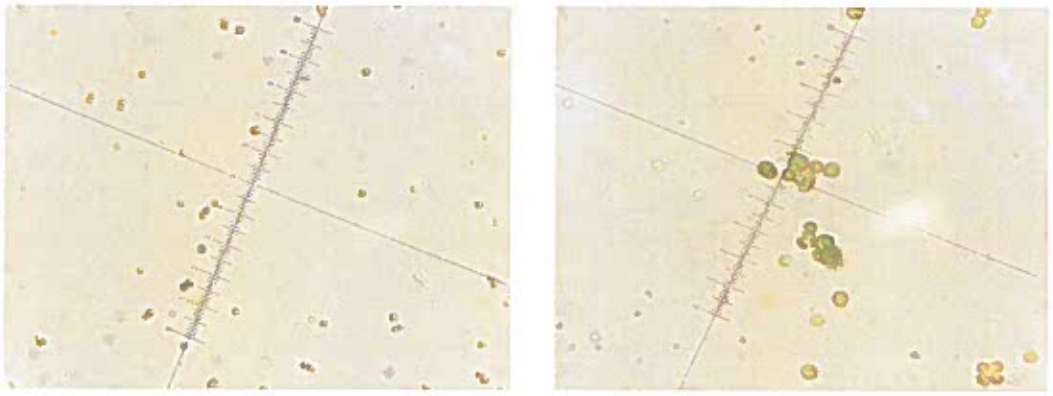

Figure 13: (A) 40x magnification of *Parachlorella kessleri* cells imaged with Leica DMR microscope. With the 40x objective, one unit is 2.5 μm. (B) 100x magnification. With the 100x objective, one unit is 1 μm.

4.11 Lipid Analysis of *Parachlorella kessleri*

A

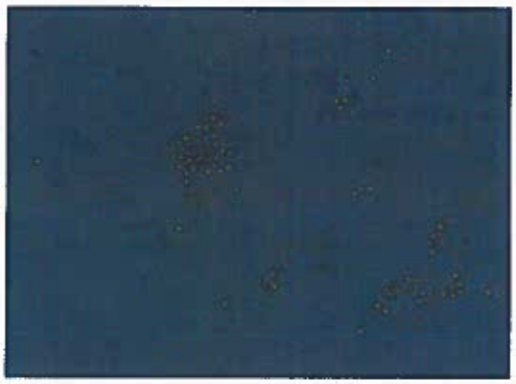

B

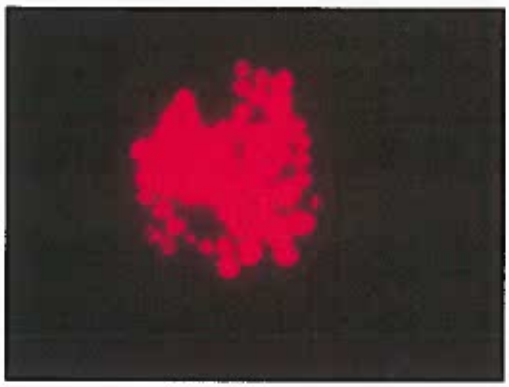

C

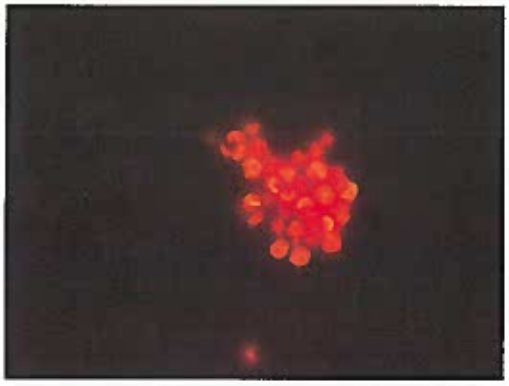

D

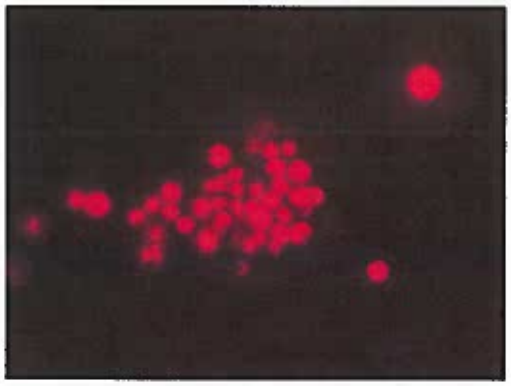

E

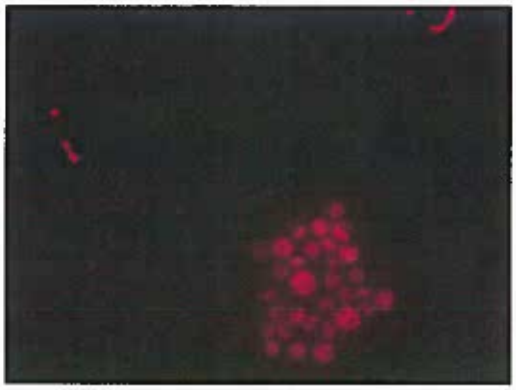

Figure 14 : (A) 35-day old algal cells grown on medium salt shaking 3N-BBM+V imaged with the standard light. (B) Unstained algal cells imaged with filter cube 3. (C) Stained algal cells imaged with filter cube 3. (D) Unstained algal cells imaged with filter cube 4. (E) Stained algal cells imaged with filter cube 4. Filter cube 3 is the Fluorescein. Filter cube 4 is the Rhodamine.

In figure C, gold-yellow emission displayed intracellular neutral lipid droplets of *Parachlorella kessleri*. In figures B and D, unstained algal cells can be seen in red. In figure E, the red colour displayed the polar membrane lipids which they emit reddish light under the rhodamine (Kolmakov et al., 2010)

On the TLC plate, spots which have migrated less, in other words, spots which have the lowest Rf value (Rf: 0.12) displayed more polar lipid molecules than fatty acids or triacylglycerols such as phospholipids or glycolipids. Spots which have medium Rf values (Rf: 0.34) displayed partial polar lipid molecules such as fatty acids. Spots which have migrated the most in other words spots which have the highest Rf value (Rf: 0.89) displayed non-polar lipid molecules such as triacylglycerols.

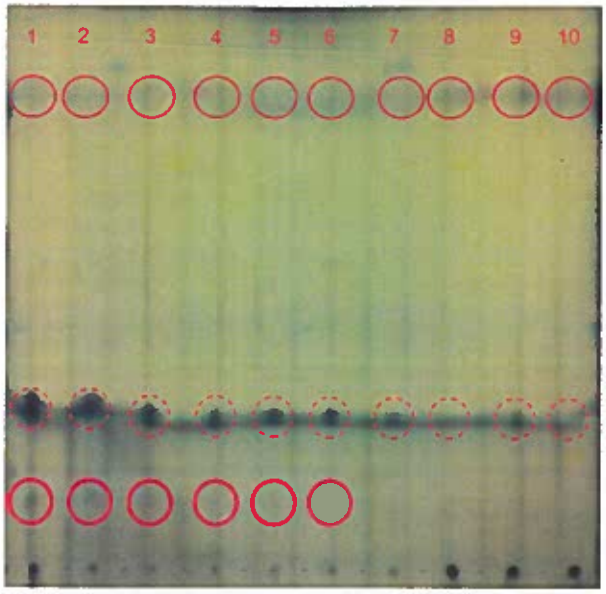

Figure 15: Thin layer chromatography results of the extracted lipids of the shaking algal cultures cultivated on no salt, low salt, and medium salt 3N-BBM+V. (1) Sunflower seed oil. (2) 1:10 dilution of sunflower seed oil. (3) 1:20 dilution of sunflower seed oil. (4) 1:30 dilution of sunflower seed oil. (5) 1:40 dilution of sunflower seed oil. (6) 1:50 dilution of sunflower seed oil. (7) 1:100 dilution of sunflower seed oil. (8) Algal culture cultivated on no salt 3N-BBM+V. (9) Algal culture cultivated on medium salt 3N-BBM+V. (10) Algal culture cultivated on low salt 3N-BBM+V.

Phospholipids or glycolipids could not be quantified in any algal samples and 1:100 diluted sunflower oil. On the other hand, they could be quantified in more concentrated sunflower oil samples. Fatty acids could be quantified in all samples. Algal cells cultivated on medium salt 3N-BBM+V had the highest amount of fatty acids. Algal cells cultivated on low salt 3N-BBM+V had the moderate amount of fatty acids. Algal cells cultivated on no salt 3N-BBM+V had the lowest amount of fatty acids among all samples. triacylglycerols could be quantified in all samples. Algal cells cultivated on the medium salt 3N-BBM+V had the highest amount of triacylglycerols. Algal cells cultivated on low salt 3N-BBM+V had the moderate amount of triacylglycerols. Algal cells cultivated on no salt 3N-BBM+V had the lowest amount of triacylglycerols among all algal samples.

A

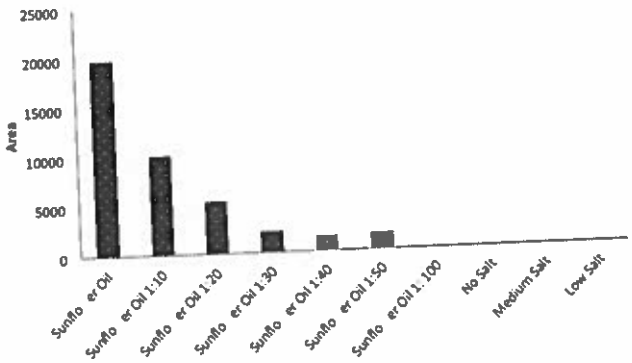

B

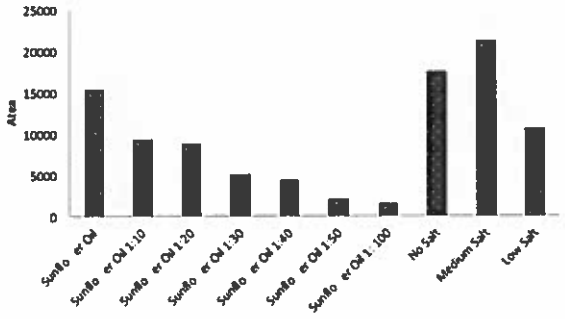

C

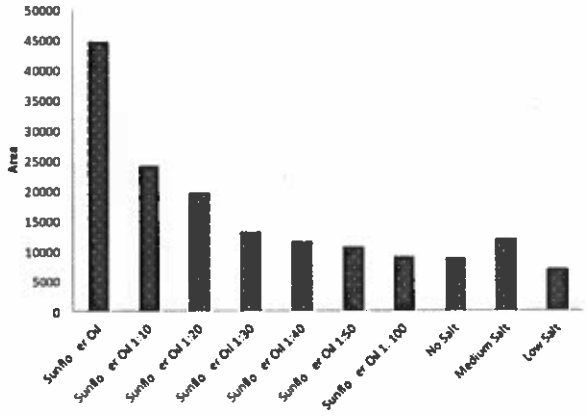

Figure 16: Densitometry data of the lipid molecules on the TLC plate. Spots were quantified by the ImageJ software. (A) Densitometry data of the phospholipid or glycolipid spots. (B) Densitometry data of the fatty acid spots. (C) Densitometry data of the triacylglycerol spots.

4.12 Phylogenetic Analysis of the *rbcL* and *accD* genes and tree construction

Using the *rbcL* protein from *Parachlorella kessleri* as the reference in protein-protein BLAST, the highest identity (99%) and total score (978) was shared with the *rbcL*

protein of *Chlorella vulgaris.* For the accD protein, the highest identity (80%) and total score (699) was shared with the *accD* protein of *Dicloster acuatus.*

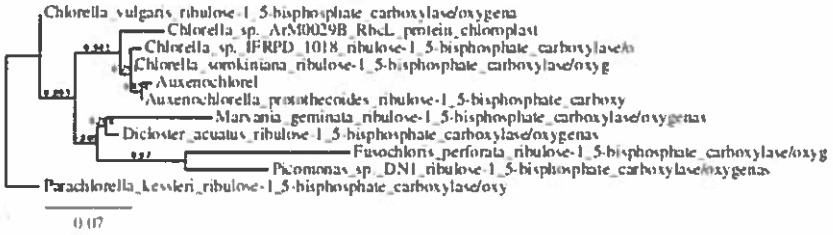

Figure 17: The phylogenetic tree from the alignment of the *Parachlorella kessleri rbcL* protein with nine most significant homologs in *Chlorella vulgaris*, *Dicloster acuatus*, *Chlorella sp. ArM0029B*, *Auxenochlorella pyrenoidosa*, *Chlorella sorokiniana*, *Auxenochlorella protothecoides*, *Chlorella sp. IFRPD 1018*, *Marvania geminata*, *Picomonas sp. DN1* and *Fusochloris perforata* was generated by Phylogeny.fr using default settings in "one click" mode. The branch length is proportional to the number of substitutions per site.

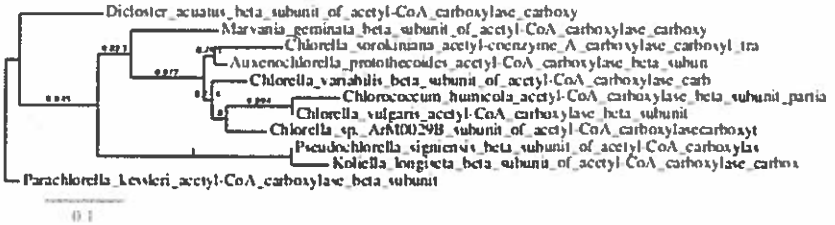

Figure 18: The phylogenetic tree from the alignment of the *Parachlorella kessleri accD* protein with nine most significant homologs in *Dicloster acuatus*, *Chlorococcum humicola*, *Marvania geminata*, *Chlorella vulgaris*, *Chlorella sp. ArM0029B*, *Chlorella variabilis*, *Auxenochlorella protothecoides*, *Chlorella sorokiniana*, *Pseudochlorella signiensis* and *Koliella longiseta* was generated by Phylogeny.fr using default settings in "one click" mode. The branch length is proportional to the number of substitutions per site.

5. Discussion

The strong positive correlation between mean total chlorophyll and optical density at 750 nm in all samples showed that the increase in mean total chlorophyll was parallel to the cell growth. Regarding the time dependent total chlorophyll analysis of still algal cultures on bold basal media in different salinity, the start time of the logarithmic phase was correlated with the increase in salinity. For instance, the growth rate of no salt 3N-BBM+V cultures in the second week was almost equal to the growth rate of medium salt 3N-BBM+V cultures in the fifth week. This was probably due to the acclimation process of cells when they faced high salinity. A likely reason behind the inability to culture *P. Kessleri* in high salt 3N-BBM+V was the osmotic shock on microalgae. Salinity dependent osmotic shock may break the cell wall and cause cell disruption (Glasby et al., 2005). Regarding the fold expression analysis, it was inferred that low salt still conditions caused *P. Kessleri* cells to increase their *accD* and *rbcL* expressions. On the other hand, medium and high salt conditions did not affect the expression of *rbcL* but caused a decrease in the *accD* gene in both cultures.

Regarding the findings of the time dependent total chlorophyll analysis of still and shaking algal cultures on 3N-BBM+V, shaking cultures have a higher total chlorophyll growth rate than still cultures. On the other hand, there was no significant difference in expression of the *rbcL* and *accD* genes. There are some potential reasons behind this result. First of all, shaking might induce the expression of other photosynthesis related genes. Secondly, shaking the cultures might just affect the cell proliferation, not the gene expression. Higher cell mass might cause detection of a higher chlorophyll content.

Regarding the time dependent total chlorophyll analysis of shaking algal cultures on bold basal media in different salinity, the ranking of the growth rate did not change. Interestingly, shaking cultures on low salt 3N-BBM+V displayed a lower growth rate than still cells on low salt 3N-BBM+V. Gene expression profile was very different from the low salt still cells as well. Shaking and low salt conditions caused *P. kessleri* cells to have a lower expression level of *accD* and *rbcL* compared to the shaking and no salt conditions. Shaking cultures on medium salt 3N-BBM+V displayed a higher growth rate than still cells on medium salt 3N-BBM+V. Also, there was a correlation between total chlorophyll growth rate and relative fold expression. Medium salt and shaking conditions caused *P. Kessleri* cells to increase their *accD* and *rbcL* expressions. In summary, shaking and salinity combination changed the whole gene expression profile.

When algal cells were transferred from the no salt /low salt 3N-BBM+V to the high salt 3N-BBM+V, they were unable to grow. This experiment was done in order to examine the acclimation trend of *P. Kessleri*. In accordance with the first experiment, we could infer that high salinity prevented algal growth. Again, the probable reason behind the inability to culture *P. Kessleri* in high salt 3N-BBM+V was the osmotic shock on microalgae. Cells endured the salinity up to 0.3 M but 0.6 M was disruptive. Regarding the gene expression profile, it was inferred that high salt conditions caused *P. Kessleri* cells to decrease their *accD* and *rbcL* expressions. Combining the results of the first and this experiment, it can be inferred that high salt conditions were correlated with the decrease in expression of the *accD* gene. On the other hand, still cultivation on high salt 3N-BBM+V did not affect the expression of rbcL, but when the cells were transferred from low salt to high salt 3N-BBM+V and cultivated on

rotary, a decrease was seen in the relative expression of rbcL as well. The potential reason of this alteration might be the individual effects of shaking or salinity change. In addition, the combinatorial effect might also cause this alteration.

There are very different types of lipid molecules found in microorganisms. On the TLC plate, 3 different types of lipids were detected; polar, partial polar and nonpolar lipids. The substance which had lower Rf value displayed polar lipids. The reason for defining them as phospholipids or glycolipids was due to the fact that sunflower seed oil contains a particular amount of these polar lipid molecules (Carelli et al., 1997). The strong polarity of phospholipids or glycolipids made them suitable candidates. The substance which had moderate Rf value displayed fatty acids. In addition, *rbcL* and *accD* genes are highly associated with fatty acid biosynthesis and their expressions were correlated with the lipid densitometry results. The substance which had the highest Rf value displayed triacylglycerols. Sunflower seed and microalgae contain a high amount of these nonpolar lipid molecules (Singh et al., 2010). In addition, *rbcL* and *accD* are highly connected with triacylglycerol biosynthesis and their expressions were correlated with the lipid densitometry results.

Lipid quantification results were also correlated with the fold expression analysis of shaking algal cells on 3N-BBM+V in different salinity. Algal cells cultivated on medium salt 3N-BBM+V had the highest amount of fatty acids and triacylglycerols. Fold expression analysis also displayed an increase in fold expression of both genes. Algal cells cultivated on low salt 3N-BBM+V had the lowest amount of fatty acids and triacylglycerols among all algal cultures. Fold expression analysis also displayed a decrease in fold expression of both genes. Phospholipids or glycolipids could not be

quantified in any algal samples and 1:100 diluted sunflower oil. The reason of not quantifying phospholipids or glycolipids in any algal samples might be a very low amount of phospholipids or glycolipids accumulation in cells.

During algal cultivation, no fungal contamination was detected by naked eye and light microscope; but due to the frequent sampling and high amount of substrate, a particular amount of contamination was inevitable. Depending on the severity of the contamination, deviations in the absorbance readings could be seen. For further studies, *P. kessleri* samples can be filtered before testing. The average size of *P. Kessleri* was around 3-6 μm. Microscopy analysis showed that there was no algal cell larger than 10 μm diameter. 20-micron filter can be effective in order to discard bigger contaminants. For smaller contaminants, 1-micron filter can be used.

As RNA yield was very low, no RNA left after LiCI precipitation of some samples for the RNA purification. Even pellet volumes were maximized, the yield was quite low. On the other hand, LiCI precipitation was very effective for the purification. Before the LiCI precipitation, A_{260}/A_{280} values of RNA the extracts were changing from 0.99 to 2.20. After the precipitation, A_{260}/A_{280} values of the RNA extracts were very close to 1.80. For further studies, larger scale of cultivation can be used to extract more RNA.

Using the same amount of RNA for cDNA production gave more reliable results in RT-qPCR. However, small/degraded RNA molecules might affect the readings. For further studies, cells can be washed with Phosphate-buffered saline before the

TRIsure extraction. This method helps prevent RNA degradation by stabilizing the pH and osmolarity in bacteria. It will also separate clumped cells (Zhao et al., 2004).

The use of oligo(dT) primer might affect the cDNA synthesis because chloroplast and ribosomal RNAs are not polyadenylated (Rott et al., 2003). Since oligo(dT) primers anneal to the poly(A) tails on the 3' end of the RNA molecule and start the cDNA synthesis, RNA molecules which do not have poly(A) tails may decrease the specificity of the primers (Thermo Fisher Scientific, 2017). In contrast to oligo(dT) primers, random primers do not need poly(A) tails and they may be more suitable for reverse transcription of RNAs which do not have poly(A) tails such as chloroplast and ribosomal RNAs. There might also be a problem in the NanoDrop readings of the samples. NanoDrop Spectrophotometer can not exclude unincorporated nucleotides in the samples. For the next time, a nucleotide removal or PCR purification kit can be used to discard unincorporated nucleotides and salts. In this way, PCR products which are below 100 bp size and free nucleotides can be attached to spin columns and discarded (QIAGEN, 2017).

For lipid extraction, Folch method was used. In order to obtain the lipid spots on the TLC plate, the final volume was decreased to 100 µL by nitrogen. This means that our extracted lipids were not concentrated enough in 1 mL sample volume. For further studies, more effective lipid extraction methods can be used on *P. Kessleri*. For example, a new lipid extraction method allows at least five times higher sample throughput (Axelsson and Gentili, 2014).

Some parameters were changed in order to obtain more definite spots on TLC plate. First of all, 5% molybdophosphoric acid was more effective than 10% molybdophosphoric acid. Secondly, dipping the plate into the acid for a few seconds gave more clear spots than spraying. On the other hand, leaving the plate in the acid more than 30 seconds caused the TLC plate to be very dark. Finally, leaving the plate in the oven for 15 min at 100 °C was more effective than 5 min at 80 °C.

6. Conclusion

This study contributes the understanding of the effects of salinity and shaking on cellular and chlorophyll content growth of *P. kessleri*. Except for the *rbcL* and *accD* genes, there are many genes which are relevant to lipid metabolism. For further studies, diacylglycerol O-acyltransferase (*DGAT*) gene can be included in the expression analysis. This gene is highly associated with lipid metabolism (Cases et al., 1998) and new correlations can be deducted by comparing the fold expression of *DGAT* gene with the densities of different types of lipid molecules. For example, *DGAT* gene is highly associated with phospholipid metabolism (Banaś et al., 2013). For further studies, new environmental stress conditions can be set in order to induce the expression of *DGAT* gene. In this way, phospholipid yield can be increased. In this study, cultures were shaken at 100 rpm. For the next time, different rpm values can be tried. In addition, the combinatorial effect of salinity and shaking should be examined in more detail. Salinity gradient can be changed as ranging from 0.1 M to 0.5 M NaCl to obtain more variable results. Finally, different chromatography methods such as gas chromatography will help us profile lipids more precisely.

7. Acknowledgements

First of all, I would like to thank my Project supervisor Dr. Ethan Hack for his endless help and advice. During my research, he taught me multidirectional scientific thinking discipline and comparative result interpretation methods. Secondly, I would like to thank laboratory manager Roselyn Brown, laboratory technicians Miriam Earnshaw, Dr. Matthew Peake and Ph.D. student Belinda Njumo for their technical assistance and moral support. Finally, I would like to express my deepest gratitude to the Newcastle University School of Biology for their courtesy and helpfulness.

8. References

Amin, S., 2009. Review on biofuel oil and gas production processes from microalgae. *Energy conversion and management, 50*(7), pp.1834-1840.

Axelsson, M. and Gentili, F., 2014. A single-step method for rapid extraction of total lipids from green microalgae. *PLoS One, 9*(2), p.e89643.

Banaś, W., Garcia, A.S., Banaś, A. and Stymne, S., 2013. Activities of acyl-CoA: diacylglycerol acyltransferase (DGAT) and phospholipid: diacylglycerol acyltransferase (PDAT) in microsomal preparations of developing sunflower and safflower seeds. *Planta, 237*(6), pp.1627-1636.

Borowitzka, M.A., 1999. Commercial production of microalgae: ponds, tanks, tubes and fermenters. *Journal of biotechnology, 70*(1), pp.313-321.

Breuer, G., Lamers, P.P., Martens, D.E., Draaisma, R.B. and Wijffels, R.H., 2013. Effect of light intensity, pH, and temperature on triacylglycerol (TAG) accumulation induced by nitrogen starvation in Scenedesmus obliquus. *Bioresource technology, 143*, pp.1-9.

Brown, M.R. and Bold, H.C., 1964. Phycological Studies Comparitive studies of the algal genera Tetracystis and Cholorococcum.

Carelli, A.A., Brevedan, M.I. and Crapiste, G.H., 1997. Quantitative determination of phospholipids in sunflower oil. *Journal of the American Oil Chemists' Society, 74*(5), pp.511-514.

Cases, S., Smith, S.J., Zheng, Y.W., Myers, H.M., Lear, S.R., Sande, E., Novak, S., Collins, C., Welch, C.B., Lusis, A.J. and Erickson, S.K., 1998. Identification of a gene encoding an acyl CoA: diacylglycerol acyltransferase, a key enzyme in triacylglycerol synthesis. *Proceedings of the National Academy of Sciences, 95*(22), pp.13018-13023.

Central Intelligence Agency. 2017. *The World Factbook.* [ONLINE] Available at: https://www.cia.gov/library/publications/the-world-factbook/geos/xx.html. [Accessed 27 June 2017]

Cheng, K.C. and Ogden, K.L., 2011. Algal biofuels: the research. *Chemical Engineering Progress, 107*(3), pp.42-47.
Chisti, Y., 2007. Biodiesel from microalgae. *Biotechnology advances, 25*(3), pp.294-306.

Chrismadha, T. and Borowitzka, M.A., 1994. Effect of cell density and irradiance on growth, proximate composition and eicosapentaenoic acid production of Phaeodactylum tricornutum grown in a tubular photobioreactor. *Journal of Applied Phycology, 6*(1), pp.67-74.

Cirulis, J.T., Strasser, B.C., Scott, J.A. and Ross, G.M., 2012. Optimization of staining conditions for microalgae with three lipophilic dyes to reduce precipitation and fluorescence variability. *Cytometry Part A, 81*(7), pp.618-626.

Depeint, F., Bruce, W.R., Shangari, N., Mehta, R. and O'Brien, P.J., 2006. Mitochondrial function and toxicity: role of the B vitamin family on mitochondrial energy metabolism. *Chemico-biological interactions, 163*(1), pp.94-112.

Fernandes, B., Teixeira, J., Dragone, G., Vicente, A.A., Kawano, S., Bišová, K., Přibyl, P., Zachleder, V. and Vítová, M., 2013. Relationship between starch and lipid accumulation induced by nutrient depletion and replenishment in the microalga Parachlorella kessleri. *Bioresource technology, 144*, pp.268-274.

Folch, J., Lees, M. and Sloane Stanley, G.H., 1957. A simple method for the isolation and purification of total lipids from animal tissues. *J biol Chem, 226*(1), pp.497-509.

Friedl, T., 1995. Inferring taxonomic positions and testing genus level assignments in coccoid green lichen algae: a phylogenetic analysis of 18S ribosomal RNA sequences from Dictyochloropsis reticulata and from members of the genus Myrmecia (Chlorophyta, Trebouxiophyceae cl. nov.) 1. *Journal of Phycology, 31*(4), pp.632-639.

Garay, L.A., Boundy-Mills, K.L. and German, J.B., 2014. Accumulation of high-value lipids in single-cell microorganisms: a mechanistic approach and future perspectives. *Journal of agricultural and food chemistry, 62*(13), pp.2709-2727.

Glasby, T.M., Creese, R.G. and Gibson, P.T., 2005. Experimental use of salt to control the invasive marine alga Caulerpa taxifolia in New South Wales, Australia. *Biological Conservation, 122*(4), pp.573-580.

Hase, R., Oikawa, H., Sasao, C., Morita, M. and Watanabe, Y., 2000. Photosynthetic production of microalgal biomass in a raceway system under greenhouse conditions in Sendai city. *Journal of bioscience and bioengineering, 89*(2), pp.157-163.

Hernández-Torres, A., Zapata-Morales, A.L., Alfaro, A.E.O. and Soria-Guerra, R.E., 2016. Identification of gene transcripts involved in lipid biosynthesis in Chlamydomonas reinhardtii under nitrogen, iron and sulfur deprivation. *World Journal of Microbiology and Biotechnology, 32*(4), p.1.

International Energy Agency. 2014. *Fossil fuel energy consumption*. [ONLINE] Available at: http://www.iea.org/statistics/statisticssearch/. [Accessed 27 June 2017].

Jose, J. and Burgess, K., 2006. Benzophenoxazine-based fluorescent dyes for labeling biomolecules. *Tetrahedron, 62*(48), pp.11021-11037.

Kaewkannetra, P., Enmak, P. and Chiu, T., 2012. The effect of CO2 and salinity on the cultivation of Scenedesmus obliquus for biodiesel production. *Biotechnology and bioprocess engineering, 17*(3), pp.591-597.

Kirrolia, A., Bishnoi, N.R. and Singh, R., 2012. Effect of shaking, incubation temperature, salinity and media composition on growth traits of green microalgae Chlorococcum sp. *J Algal Biom Utlzn*, 3, pp.46-53.

Kirst, G.O., 1990. Salinity tolerance of eukaryotic marine algae. *Annual review of plant biology, 41*(1), pp.21-53.

Kolmakov, K., Belov, V.N., Bierwagen, J., Ringemann, C., Müller, V., Eggeling, C. and Hell, S.W., 2010. Red - emitting rhodamine dyes for fluorescence microscopy and nanoscopy. *Chemistry-A European Journal, 16*(1), pp.158-166.

Lei, A., Chen, H., Shen, G., Hu, Z., Chen, L. and Wang, J., 2012. Expression of fatty acid synthesis genes and fatty acid accumulation in Haematococcus pluvialis under different stressors. *Biotechnology for Biofuels, 5*(1), p.18.

Li, X., Přibyl, P., Bišová, K., Kawano, S., Cepák, V., Zachleder, V., Čížková, M., Brányiková, I. and Vítová, M., 2013. The microalga Parachlorella kessleri—A novel highly efficient lipid producer. *Biotechnology and Bioengineering, 110*(1), pp.97-107.

Li, Y., Chen, Y.F., Chen, P., Min, M., Zhou, W., Martinez, B., Zhu, J. and Ruan, R., 2011. Characterization of a microalga Chlorella sp. well adapted to highly concentrated municipal wastewater for nutrient removal and biodiesel production. *Bioresource technology, 102*(8), pp.5138-5144.

Li, Y., Horsman, M., Wang, B., Wu, N. and Lan, C.Q., 2008. Effects of nitrogen sources on cell growth and lipid accumulation of green alga Neochloris oleoabundans. *Applied microbiology and biotechnology, 81*(4), pp.629-636.

Li, Y., Naghdi, F.G., Garg, S., Adarme-Vega, T.C., Thurecht, K.J., Ghafor, W.A., Tannock, S. and Schenk, P.M., 2014. A comparative study: the impact of different

lipid extraction methods on current microalgal lipid research. *Microbial cell factories, 13*(1), p.14.

Lu, Y., Kong, R. and Liu, J., 2012. Cloning and expression analysis of accD gene in Chlorella protothecoides FACHB-2. *African Journal of Microbiology Research, 6*(49), pp.7545-7549.

Mata, T.M., Martins, A.A. and Caetano, N.S., 2010. Microalgae for biodiesel production and other applications: a review. *Renewable and sustainable energy reviews, 14*(1), pp.217-232.

Metting, F.B., 1996. Biodiversity and application of microalgae. *Journal of industrial microbiology, 17*(5-6), pp.477-489.

Minhas, A.K., Hodgson, P., Barrow, C.J. and Adholeya, A., 2016. A review on the assessment of stress conditions for simultaneous production of microalgal lipids and carotenoids. *Frontiers in microbiology, 546*(7), pp.10-11.

Minnikin, D.E., O'donnell, A.G., Goodfellow, M., Alderson, G., Athalye, M., Schaal, A. and Parlett, J.H., 1984. An integrated procedure for the extraction of bacterial isoprenoid quinones and polar lipids. *Journal of Microbiological Methods, 2*(5), pp.233-241.

Moser, B.R., 2009. Biodiesel production, properties, and feedstocks. *In Vitro Cellular & Developmental Biology-Plant, 45*(3), pp.229-266.

Nichols, H.W. and Bold, H.C., 1965. Trichosarcina polymorpha gen. et sp. nov. *Journal of Phycology, 1*(1), pp.34-38.

Ota, S., Oshima, K., Yamazaki, T., Kim, S., Yu, Z., Yoshihara, M., Takeda, K., Takeshita, T., Hirata, A., Bišová, K. and Zachleder, V., 2016. Highly efficient lipid production in the green alga Parachlorella kessleri: draft genome and transcriptome endorsed by whole-cell 3D ultrastructure. *Biotechnology for biofuels, 9*(1), p.13.

Piasecka, A., Krzemińska, I. and Tys, J., 2017. Enrichment of Parachlorella kessleri biomass with bioproducts: oil and protein by utilization of beet molasses. *Journal of Applied Phycology, 29*(4), pp.1-9.

Přibyl, P., Cepák, V. and Zachleder, V., 2012. Production of lipids in 10 strains of Chlorella and Parachlorella, and enhanced lipid productivity in Chlorella vulgaris. *Applied microbiology and biotechnology, 94*(2), pp.549-561.

Proposal for a directive of the European Parliment and of the Council on the promotion of the use of energy from renewable sources (recast). (2017). [ebook] Brussels: European Commission. Available at: https://ec.europa.eu/energy/sites/ener/files/documents/1_en_act_part1_v7_1.pdf [Accessed 11 Jun. 2017].

QIAGEN. 2017. DNA Clean Up. [ONLINE] Available at: https://www.qiagen.com/us/shop/sample-technologies/dna/dna-clean-up/qiaquick-pcr-purification-kit/#orderinginformation. [Accessed 1 August 2017].

Read, B.A. and Tabita, F.R., 1994. High Substrate Specificity Factor Ribulose Bisphosphate Carboxylase/Oxygenase from Eukaryotic Marine Algae and Properties of Recombinant Cyanobacterial Rubisco Containing "Algal" Residue Modifications. *Archives of Biochemistry and Biophysics, 312*(1), pp.210-218.

Reuveni, M., Agapov, V. and Reuveni, R., 1996. Controlling powdery mildew caused by Sphaerotheca fuliginea in cucumber by foliar sprays of phosphate and potassium salts. *Crop Protection, 15*(1), pp.49-53.

Rostek, E. and Biernat, K., 2012. Analysis of the quality parameters of selected motor biofuels, taking into account the current requirements of the worldwide fuel charter. *Journal of KONES, 19*(2), pp.449-458.

Rott, R., Zipor, G., Portnoy, V., Liveanu, V. and Schuster, G., 2003. RNA polyadenylation and degradation in cyanobacteria are similar to the chloroplast but different from Escherichia coli. *Journal of Biological Chemistry, 278*(18), pp.15771-15777.

Rubio, V., Linhares, F., Solano, R., Martín, A.C., Iglesias, J., Leyva, A. and Paz-Ares, J., 2001. A conserved MYB transcription factor involved in phosphate starvation signaling both in vascular plants and in unicellular algae. *Genes & development, 15*(16), pp.2122-2133.

Rupérez, P., 2002. Mineral content of edible marine seaweeds. *Food chemistry, 79*(1), pp.23-26.

Scottish Association for Marine Science. 2014. *List of media used to maintain strains at CCAP*. [ONLINE] Available at: https://www.ccap.ac.uk/pdfrecipes.htm. [Accessed 1 July 2017].

Singh, A. and Olsen, S.I., 2011. A critical review of biochemical conversion, sustainability and life cycle assessment of algal biofuels. *Applied Energy, 88*(10), pp.3548-3555.

Singh, A., Nigam, P.S. and Murphy, J.D., 2011. Renewable fuels from algae: an answer to debatable land based fuels. *Bioresource technology, 102*(1), pp.10-16.

Singh, S.P. and Singh, D., 2010. Biodiesel production through the use of different sources and characterization of oils and their esters as the substitute of diesel: a review. *Renewable and sustainable energy reviews, 14*(1), pp.200-216.

Spencer, C.P., 1957. Utilization of trace elements by marine unicellular algae. *Microbiology, 16*(1), pp.282-285.

Spolaore, P., Joannis-Cassan, C., Duran, E. and Isambert, A., 2006. Commercial applications of microalgae. *Journal of bioscience and bioengineering, 101*(2), pp.87-96.

Takagi, M. and Yoshida, T., 2006. Effect of salt concentration on intracellular accumulation of lipids and triacylglyceride in marine microalgae Dunaliella cells. *Journal of bioscience and bioengineering, 101*(3), pp.223-226.

Thermo Fisher Scientific. 2017. Reverse Transcription Reaction Setup. [ONLINE] Available at: https://www.thermofisher.com/uk/en/home/life-science/cloning/cloning-learning-center/invitrogen-school-of-molecular-biology/rt-education/reverse-transcription-setup.html. [Accessed 1 August 2017]

University of Minnesota, The Springer Lab. 2015. Lithium Chloride RNA Cleanup Protocol. [ONLINE] Available at: https://cbs.umn.edu/springer-lab/lithiumchloride. [Accessed 15 July 2017]

World Energy Council. 2016. *World Energy Resources*. [ONLINE] Available at: https://www.worldenergy.org/wp-content/uploads/2016/10/World-Energy-Resources-Full-report-2016.10.03.pdf. [Accessed 27 June 2017].

Yocum, C.F., 2008. The calcium and chloride requirements of the O 2 evolving complex. *Coordination Chemistry Reviews, 252*(3), pp.296-305.

Zhao, X., Hilliard, L.R., Mechery, S.J., Wang, Y., Bagwe, R.P., Jin, S. and Tan, W., 2004. A rapid bioassay for single bacterial cell quantitation using bioconjugated nanoparticles. *Proceedings of the National Academy of Sciences of the United States of America, 101*(42), pp.15027-15032.

Appendix I

Component	Added amount in 1000 ml water
NaNO3	25.0 g
CaCl2.2H2O	2.5 g
MgSO4.7H2O	7.5 g
K2HPO4.3H2O	7.5 g
KH2PO4	17.5 g
Trace element solution	
Na2EDTA	0.75 g
FeCl3.6H2O	97.0 mg
MnCl2.4H2O	41.0 mg
ZnCl2	5.0 mg
CoCl2.6H2O	2.0 mg
Na2MoO4.2H2O	4.0 mg
Vitamin B1	1,2 g
Vitamin B12	1.0 g